NATURAL RESOURCES

GEOLOGIC MAP OF THE OAKVILLE AND RAINBOW FALLS 7.5-MINUTE QUADRANGLES, LEWIS, THURSTON, AND GRAYS HARBOR COUNTIES, WASHINGTON

by Michael Polenz, Catherine Samson, Tabor Reedy, Wesley von Dassow, W. Cody Duckworth, Todd R. Lau, Megan L. Anderson, Elizabeth A. Nesbitt, Jeffrey H. Tepper, S. Andrew DuFrane, and Gabriel Legoretta Paulín

WASHINGTON
GEOLOGICAL SURVEY
Map Series 2020-02
December 2020

INTERNALLY REVIEWED

WASHINGTON STATE DEPARTMENT OF
NATURAL RESOURCES
WASHINGTON GEOLOGICAL SURVEY

GEOLOGIC MAP OF THE OAKVILLE AND RAINBOW FALLS 7.5-MINUTE QUADRANGLES, LEWIS, THURSTON, AND GRAYS HARBOR COUNTIES, WASHINGTON

by Michael Polenz, Catherine Samson, Tabor Reedy, Wesley von Dassow, W. Cody Duckworth, Todd R. Lau, Megan L. Anderson, Elizabeth A. Nesbitt, Jeffrey H. Tepper, S. Andrew DuFrane, and Gabriel Legoretta Paulín

WASHINGTON
GEOLOGICAL SURVEY
Map Series 2020-02
December 2020

This geologic map was funded in part by the USGS National Cooperative Geologic Mapping Program, award no. G19AC00220

This publication has been subject to an iterative technical review process by at least one Survey geologist who is not an author. This publication has also been subject to an iterative review process with Survey editors and cartographers.

WASHINGTON STATE DEPARTMENT OF
NATURAL RESOURCES
WASHINGTON GEOLOGICAL SURVEY

DISCLAIMER

Neither the State of Washington, nor any agency thereof, nor any of their employees, makes any warranty, express or implied, or assumes any legal liability or responsibility for the accuracy, completeness, or usefulness of any information, apparatus, product, or process disclosed, or represents that its use would not infringe privately owned rights. Reference herein to any specific commercial product, process, or service by trade name, trademark, manufacturer, or otherwise, does not necessarily constitute or imply its endorsement, recommendation, or favoring by the State of Washington or any agency thereof. The views and opinions of authors expressed herein do not necessarily state or reflect those of the State of Washington or any agency thereof.

INDEMNIFICATION

Research supported by the U.S. Geological Survey, National Cooperative Geologic Mapping Program, under USGS award number G19AC00220. The views and conclusions contained in this document are those of the authors and should not be interpreted as necessarily representing the official policies, either expressed or implied, of the U.S. Government.

WASHINGTON STATE DEPARTMENT OF NATURAL RESOURCES

Hilary S. Franz—*Commissioner of Public Lands*

WASHINGTON GEOLOGICAL SURVEY

Casey R. Hanell—State Geologist
Jessica C. Czajkowski—Assistant State Geologist
Ana Shafer—Assistant State Geologist

Washington State Department of Natural Resources
Washington Geological Survey

Mailing Address:
MS 47007
Olympia, WA 98504-7007

Street Address:
Natural Resources Bldg, Rm 148
1111 Washington St SE
Olympia, WA 98501

Phone: 360-902-1450
Fax: 360-902-1785
Email: geology@dnr.wa.gov
Website: http://www.dnr.wa.gov/geology

Publications and Maps:
www.dnr.wa.gov/programs-and-services/geology/publications-and-data/publications-and-maps

Washington Geology Library Searchable Catalog:
www.dnr.wa.gov/programs-and-services/geology/washington-geology-library

Suggested Citation: Polenz, Michael; Samson, Catherine; Reedy, Tabor; von Dassow, Wesley; Duckworth, C. W.; Lau, T. R.; Anderson, M. L.; Nesbitt, E. A.; Tepper, J. H.; DuFrane, S. A.; Legoretta Paulín, Gabriel, 2020, Geologic map of the Oakville and Rainbow Falls 7.5-minute quadrangles, Lewis, Thurston, and Grays Harbor Counties, Washington: Washington Geological Survey Map Series 2020-02, 1 sheet, scale 1:24,000, 19 p. text. [http://www.dnr.wa.gov/publications/ger_ms2020-02_geol_map_oakville_rainbow_falls_24k.zip]

© 2020 Washington Geological Survey
Published in the United States of America

Contents

Introduction 1
Geologic Overview 1
Methods 2
    Geologic Mapping 2
    Geophysics 2
Description of Map Units 2
    Holocene to Pleistocene Nonglacial Deposits 2
    Pleistocene Glacial Sediments 3
    Quaternary to Eocene Continental Deposits 6
    Tertiary Volcanic and Sedimentary Bedrock 6
Whole Rock Geochemistry Results and Discussion 10
Description of Structures 12
    Named Faults 13
    Named Folds 14
    Unnamed Structures 15
Suggestions for Further Study 15
Acknowledgments 15
References 15

FIGURES

Figure 1. Lidar-based relative elevation model of the Chehalis River valley 5
Figure 2. Total alkalis vs. SiO_2 volcanic classification plot 11
Figure 3. MORB-normalized spidergram 12

TABLES

Table 1. Chemical characteristics of clasts 11

MAP SHEET

Geologic Map of the Oakville and Rainbow Falls 7.5-minute Quadrangles,
Lewis, Thurston, and Grays Harbor Counties, Washington

Figure M1. Potential field geophysical map for the Oakville and Rainbow Falls quadrangles

Geologic Map of the Oakville and Rainbow Falls 7.5-minute Quadrangles, Lewis, Thurston, and Grays Harbor Counties, Washington

by Michael Polenz[1], Catherine Samson[1], Tabor Reedy[1], Wesley von Dassow[1], W. Cody Duckworth[1], Todd R. Lau[1], Megan L. Anderson[1], Elizabeth A. Nesbitt[2], Jeffrey H. Tepper[3], S. Andrew DuFrane[4], Gabriel Legoretta Paulín[5]

[1] Washington Geological Survey
MS 47007
Olympia, WA
98504-7007

[2] The Burke Museum of Natural History and Culture
University of Washington
4300 15th Ave NE
Seattle, WA
98108-1446

[3] Department of Geology
University of Puget Sound
1500 N Warner St. #1048
Tacoma, WA
98416-1048

[4] Department of Earth and Atmospheric Sciences
University of Alberta
1-26 Earth Sciences Building
Edmonton, Alberta
Canada T6G 2E3

[5] Instituto de Geografía, Universidad Nacional Autónoma de México
Ciudad Universitaria Del Coyoacán
cp 04510, México, D.F.

ABSTRACT

The Oakville and Rainbow Falls quadrangles straddle Lewis, Thurston, and Grays Harbor Counties west of Washington's economically vital Interstate 5. This new map supports private and public resource management with insights into geologic deposits, structures, and hazards. Field- and lidar-informed mapping improves identification of landslides and other deposits. Fault architecture is interpreted from field observations, new gravity data, and, for most faults, modeling of magnetic and gravity anomalies. Abundant landslides in sedimentary rocks between the Doty and Scammon Creek faults mostly mask bedding orientations. New detrital zircon U-Pb analyses support stratigraphic revisions, notably including: (1) recognition of Miocene sedimentary rocks along the western map edge and (2) the combination of the Eocene nearshore Skookumchuck and marine McIntosh Formations into a single marine-to-deltaic unit. New geochemical analyses support mapping basalt as Crescent Formation in the Black Hills and near the confluence of Independence Creek and the Chehalis River; basalt in the Rainbow Falls quadrangle is the Sentinel Bluffs Member of the Grande Ronde Basalt (Columbia River Basalt Group). Geochemical traits of volcaniclastic pebbles in Wilkes Formation sampled near the western map edge and Astoria(?) Formation sampled near the eastern map edge suggest derivation from a mix of Crescent Formation and younger alkaline forearc lavas, both exposed west of the map area. Glacial outwash from the Vashon Stade of the Fraser Glaciation, and at least one earlier Cordilleran ice incursion, raised the Chehalis River valley floor in the Oakville quadrangle and caused aggradation in tributary valleys. The outwash and younger alluvium provide ample gravel resources and a productive aquifer that is sensitive to contamination.

INTRODUCTION

The principal land uses in the Oakville and Rainbow Falls quadrangles are forestry in the hills and agriculture in the valleys. The main population centers are located along the Chehalis River valley in the Oakville quadrangle. These include the city of Oakville and unincorporated residential areas southeast of Oakville, including the Chehalis Reservation.

This map has greatly benefitted from prior, smaller-scale mapping which focused on coal resource potential (Snavely and others, 1958), water resources (Wallace and Molenaar, 1961; Weigle and Foxworthy, 1962; Noble and Wallace, 1966), and geology (Pease and Hoover, 1957; Logan, 1987; Walsh and others, 1987; Wells and Sawlan, 2014).

Our mapping efforts focused on characterization of geologic hazards, including potentially active crustal faults as well as the role the area might play in the ongoing seismotectonics of the region. Mapping also improved identification of landslide areas. New stratigraphic insights led to a combination of the Skookumchuck and McIntosh Formations into a single map unit, and we newly recognized Miocene sedimentary bedrock along the western side of the map area. We further assessed subsurface geology and mapped distributions and locations of possible aggregate resources.

GEOLOGIC OVERVIEW

The entire map area is drained by the Chehalis River, which runs east across most of the Rainbow Falls quadrangle near the southern map edge before exiting to the south. It then reenters the map area farther north to meander west across the Oakville

quadrangle. The principal tributaries in the map area include, from north to south: Black River, Independence River, Lincoln Creek, and Bunker Creek.

The oldest exposed rocks in the map area are lower Eocene Crescent Formation basalt of the Siletzia terrane (Wells and others, 2014; Eddy and others, 2017), which was accreted to North America during the early Eocene (Eddy and others, 2016, 2017). In the map area, Crescent Formation is exposed in the Black Hills near the northern map edge and in the southern center of the Oakville quadrangle near the confluence of Independence Creek and the Chehalis River.

Sedimentary rocks within the map area document a transition from mostly marine early Eocene to mostly terrestrial later Eocene conditions, interpreted from transitions in the fossil record and sedimentary characteristics. The Lincoln Creek Formation documents a return to marine conditions from the latest Eocene through earliest Miocene. Miocene rocks document another transition from marine to terrestrial conditions, with early deposition of the marine Astoria(?) Formation followed by mostly terrestrial deposition of the Wilkes Formation.

Alpine glaciation of the Cascade Range produced Pliocene to Pleistocene outwash gravel that was deposited in lowlands west of the Cascade Range and is now found in some eastern sections of the map area.

The lower reaches of valleys are filled with Quaternary sediments, including: nonglacial alluvium, outwash from at least two incursions of Cordilleran ice masses that moved south into the Puget Lowland northeast of the map area, and alpine glacial and nonglacial sediments derived from the Cascade Range. These deposits fill the main stems and larger tributary valleys of the Chehalis and Black Rivers and Independence, Lincoln, and Bunker Creeks.

Fault-bounded uplift of the Black Hills and Lincoln Creek blocks (Fig. M1) has exposed Eocene rocks. Late Eocene and younger deposits are exposed mostly in adjacent basins. Apparent onlapping of younger Eocene sedimentary rocks onto older Eocene volcanic rocks implies Eocene paleo-topography that suggests the uplifted blocks and basins formed at least partly during the Eocene. The present structural setting has been interpreted mainly in the regional context of Miocene–present clockwise block rotation (Beck, 1984; Wells and others, 1998; Lewis and others, 2003; Wells and McCaffrey, 2013), which has led to north–south shortening in and near the map area (Wells and others, 1998; Johnson and others, 2004; McCaffrey and others, 2013).

METHODS

Geologic Mapping

We identified units from field observations in the Oakville and north half of the Rainbow Falls quadrangle in the summer and fall of 2019, and in the south half of the Rainbow Falls quadrangle in the summer and falls of 2018 and 2019. We collected field data and constructed preliminary field-based maps using ArcMap and ArcCollector. Most outcrops were small and weathered so measured features (bedding, joints, or shears) could not be traced beyond individual outcrops. We refined the field mapping through analysis of well and boring records, geotechnical reports, geophysical data, petrographic review of thin sections, prior geologic mapping and studies, aerial orthophotos, and geomorphic features identified from lidar. We used a lidar-based digital elevation model (DEM) with a 2-m grid resolution to estimate site elevations and derive hillshade images, contours, and other products. Edge mismatches with the adjacent Rochester and Adna quadrangles (Polenz and others, 2019; Sadowski and others, 2019) are intentional and are based on insights from our latest mapping endeavors. We used the geologic time scale of the United States Geological Survey (USGS) Geologic Names Committee (2010). Where that scale lacked Epoch subdivisions, we referred to Walker and Geissman (2009).

Geophysics

We supplemented Lau and others' (2018) isostatic gravity map with new gravity stations where existing data were relatively sparse or particular questions warranted a denser data set (for example, along previously mapped but not well understood faults). We applied a horizontal gradient filter to the isostatic gravity grid and used an algorithm to select linear maxima ("max spots"; Fig. M1). Washington Geologicl Survey (WGS) geophysicists used these new gravity data, recent USGS aeromagnetic data (Blakely and others, 2020), new WGS ground magnetic data, and 120 recent WGS rock density measurements to develop a potential field geophysical map for the map area (Fig. M1). We also modeled gravity and magnetic potential field profiles along lines A–A′ to D–D′ near the map area (Anderson and others, 2019) and E–E′ within the map area (Fig. M1). These geophysical data and analyses supplemented our interpretations.

DESCRIPTION OF MAP UNITS

Holocene to Pleistocene Nonglacial Deposits

af **Artificial fill (Holocene)**—Cobbles, pebbles, sand, silt, clay, and boulders, all in various amounts, engineered and non-engineered; placed to raise roadbeds and other surfaces. Excludes small or shallow fills (less than 5 ft deep) such as most road-related deposits.

ml **Modified land (Holocene)**—Locally derived soil, cobbles, pebbles, sand, silt, clay, and boulders, all in various amounts, reworked by excavation and (or) redistribution that modified topography; includes gravel pits and other developments. Excludes small or shallow reworking such as most residential site preparation and road-related modifications with excavations or deposits less than 5 ft deep or thick.

Qls **Landslide deposits (Holocene to Pleistocene)**—Sand, silt, clay, pebbles, cobbles, and boulders, all in various amounts, derived from units upslope; weathering varied; particles angular to rounded; typically loose, unsorted, and jumbled; locally stratified in blocks; mostly mapped from landforms expressed in lidar (for example,

hummocky terrain, deranged and disrupted drainages, disrupted or irregular slopes, tilted benches in hillsides, concave upper and convex lower slope forms); common in all sedimentary rock units but pervasive in those of Eocene age.

Qp **Peat (Holocene to Pleistocene)**—Peat, gyttja, muck, silt, clay, and sand in wetland areas and other flat-bottomed depressions, commonly crescent shaped in relict alluvial channels; mostly mapped from landforms expressed in lidar (for example, hummocky terrain, deranged and disrupted drainages, disrupted or irregular slopes, tilted benches in hillsides; concave upper and convex lower slope forms) coupled with water-loving vegetation and (or) wet conditions revealed in aerial true color and infrared photos and lidar.

Qa
Qoa
Qoa_1
Qoa_2

Alluvium (Holocene to Pleistocene)—Floodplain and channel sediments of pebbles, cobbles, boulders, sand, silt, clay, and peat, all in various amounts; gray to pale gray and brown to pale brown, weathers brown, orange, red, and yellow; generally fresh to mildly weathered but locally supplemented with proximally derived, weathered particles; loose; mostly well-rounded and moderately to well-sorted; lithologically varied, especially in the shared floodplain of the Chehalis and Black Rivers within the Oakville quadrangle where glacial outwash and the Chehalis River have contributed distally sourced rocks. In the Chehalis River valley between Rochester and Oakville, well records constrain total alluvial thickness, but that may include units Qa, Qoa, Qgo, and Qpog. Total alluvial thickness is 117 ft above shale bedrock at well W11 in the center of the valley near the eastern map edge, and Qa is likely only part of that. A 113-ft surface elevation at that location indicates that alluvium extends to slightly below contemporary mean sea level (msl). At least 161 ft of alluvium reported by Sinclair and Hirshey (1992) in a different well about 1.4 mi north of well W11 indicates a base of alluvium close to 40 ft below msl. The base of alluvium below msl implies that either the lower part is glacial outwash (deposited when sea level was lower), or the valley floor has been lowered (by tectonics or isostasy) since the onset of alluvial deposition. The alluvium in this part of the Chehalis River valley forms a highly permeable and productive, generally unconfined aquifer. These traits render the aquifer sensitive to pollution and the surface prone to drought.

Unit Qoa includes alluvial deposits that appear to be no longer receiving sediment. Bretz (1913) contended that well records indicate at least 75 ft of Chehalis valley floor aggradation by Vashon proglacial outwash at Centralia a few miles east of the map area; he suggested that tributary valleys responded by ponding and aggrading with locally derived sediment. Many benches along the sides of Lincoln Creek Valley, and a few in Independence Valley, rest about 10–25 ft above the modern valley floor, just like outwash terraces in the Chehalis River valley rise about 10–25 ft above the adjacent valley floor (Fig. 1). In addition, slope breaks at a similar height above the valley floor commonly separate relatively smooth and gentle, lower slopes from steeper and mostly rougher slopes above. These patterns suggest terraces that appear to support Bretz's inference of tributary ponding and aggradation, and the benches are tentatively mapped as (queried) unit Qoa_1.

Unit Qoa_2 identifies a set of older, more elevated benches on the south side of Independence Valley. Observed exposures of unit Qoa_2 revealed clay soil with isolated, small fragments (<1 cm) of locally derived sedimentary rock—consistent with strongly weathered alluvium, but an alluvial origin remains speculative, and all polygons of unit Qoa_2 are therefore queried. The clayey soil development in unit Qoa_2 indicates that the deposits are older than Qoa_1, and probably older than most or all of undivided unit Qoa. Undivided unit Qoa is mapped where relict alluvial deposits have not been tied to either age grouping.

Qaf
Qoaf

Alluvial fan (Holocene to Pleistocene)—Silt, sand, and gravel, all in various amounts, in broad, concentric lobes where narrow drainages spill out onto a broader, flatter valley floor; gray to brown; loose; subangular to rounded; moderately to poorly sorted; stratified to unstratified. Mostly mapped from fan-shaped landforms expressed in lidar. Unit Qoaf identifies relict deposits that no longer receive sediment.

Pleistocene Glacial Sediments

LATE PLEISTOCENE CONTINENTAL GLACIAL DEPOSITS

The Cordilleran ice sheet entered the Puget Lowland from the north during the late Wisconsinan Vashon stade (marine oxygen isotope stage 2, MIS[1]) and earlier glaciations. The Puget lobe at the southern tip of the ice reached its southern terminus a few miles east of the map area (Upham, 1904; Bretz, 1911; Lea, 1984; Polenz and others, 2018, 2019) during the Vashon and at least one earlier ice advance. Outwash (glacial meltwater

[1] MIS: global marine oxygen isotope stage curve, where even-numbered stages are used as a proxy for timing and intensity of global glacial periods (Morrison, 1991). For discussion of corresponding Cordilleran ice sheet advances into the Puget Lowland, see Booth and others (2004), Troost and Booth (2008), Polenz and others (2013, 2015), and Troost (2016). For timing of the MIS 2 ice advance into the map area at the southern limit of the Vashon glaciation, we refer to Polenz and others' (2015) fig. 3 and discussion, although the southern tip of their fig. 3 should have been extended south of Olympia to the Vashon ice limit south of Scatter Creek.

transported alluvium) is the only drift in the map area. Wallace and Molenaar's (1961) reference to "Till (?)" in a well record 0.25 mi west of Helsing Junction at or near the east edge of the Oakville quadrangle probably refers to a debris flow deposit, such as has been suggested in association with Vashon outwash east of the map area (Pringle and Goldstein, 2002; Parker and others, 2008; Pringle and Goldstein, Centralia College and Univ. of Puget Sound, respectively, written commun., 2018).

Field observations of outwash in the map area support the expectation that it resembles outwash documented in greater detail east of the map area, where deposits from successive Cordilleran ice advances (hereafter "northern-sourced" drift) largely resemble each other in lithology and structure. The provenance of the northern-sourced drift is mainly northwest Washington, British Columbia, and the Cascade Range (Polenz and others, 2019).

The Vashon-age Puget ice lobe was divided at its southern end into a western (Olympia) and eastern (Yelm) lobe (Bretz, 1913; Noble and Wallace, 1966; Walsh and Logan, 2005). Polenz and others (2019) inferred similar lobes for earlier ice advances and documented that clast assemblages associated with the Olympia lobe contain 30–60 percent basalt and 15–35 percent intermediate igneous and granitoid rocks, 5–25 percent quartz and chert, and 2–13 percent metamorphic rocks, whereas clast assemblages associated with the Yelm lobe tend to contain more intermediate igneous rocks (22–46%) at the expense of quartz, chert, basalt, and metamorphic rocks. Polenz and others (2019) further documented that the older drift is generally more weathered than Vashon drift, and that weathering of clasts within the older deposits is more varied than in Vashon drift—except where waterlogging or burial impeded weathering.

Qgo **Vashon proglacial outwash, undivided**—Pebble gravel, locally cobbly; less commonly pebbly sand or sand; well-sorted and clast-supported, locally with matrix and interbeds of silt and sand; localized diamictons not observed but suggested by a well record at or near the eastern map edge (Wallace and Molenaar, 1961) and observations east of the map area (Pringle and Goldstein, 2002; Parker and others, 2008; Polenz and others, 2018; Pringle and Goldstein, Centralia College and Univ. of Puget Sound, respectively, written commun., 2018); gray to pale gray, or mildly weathered to pale brown, brown, or variegated with iron stains; loose and commonly cohesionless; well-rounded to subrounded; moderately to well-sorted; faintly bedded or lacking bedding; lithologically diverse (see *Late Pleistocene continental glacial deposits* above).

Unit Qgo forms inselbergs of relict alluvium that typically rise 10–25 ft above the younger alluvium of the surrounding Chehalis River valley floor (Fig. 3). They record an interlude of proglacial valley floor aggradation that also ponded tributary valleys (Bretz, 1913). Unit thickness exceeds 25 ft based on that terrace height. Within the Oakville quadrangle, well records on the eastern map edge (S2 and two nearby wells interpreted by Sinclair and Hirshey, 1992; well W11) and near the western map edge (well W7) suggest similar thicknesses of alluvium (~120–160 ft) across the Chehalis River valley. But not all of this alluvium is Qgo, it also includes alluvial unit Qa and may include unit Qpo.

Unit Qgo forms flat to gently undulating surfaces, and together with units Qa and Qpog hosts a productive aquifer that is highly permeable, very well drained, generally unconfined, and thus sensitive to pollution; these traits also leave the surface prone to drought. Unit Qgo probably forms most of this aquifer because when the advancing Cordilleran ice first dammed the Strait of Juan de Fuca, thereby routing meltwater south into the Chehalis River valley, the Puget Lowland formed a proglacial sediment trap (Booth, 1994). Consequently, meltwater that entered the Chehalis River basin initially carried no bedload. Meanwhile, global sea level during the glaciation was lower than present-day sea level, and the voluminous, sediment-starved meltwater therefore had considerable erosive power in the Chehalis River valley and may have scoured the valley to below contemporary mean sea level (see also unit Qa). The fact that unit Qgo later aggraded to above the post-glacially active valley floor suggests that unit Qgo constitutes most of the alluvium in the valley.

A lack of channel meander landforms in unit Qgo (easily missed in the field but clearly expressed in Figure 1) coupled with mostly pebbly exposures on the Qgo surfaces suggests that unit Qgo was deposited in a braided(?) geomorphic setting that differs from the modern flood plain and meandering channel environment. We suggest that this braided outwash deposition was coupled, at least episodically, with much greater than modern discharge volumes that may, at times, have filled the width of the valley. That inference is supported by: bouldery outwash gravels in well records and some exposures in and east of the map area, the large volume of Cordilleran ice that filled the Puget Lowland, and episodic and historic observations of cataclysmic proglacial meltwater floods (jökulhlaups) elsewhere on earth. There is also ample evidence for similar or larger proglacial floods in the geologic record, including the Missoula floods in Washington state, and other paleohydrologic arguments based mostly on evidence east of the map area.

The age of unit Qgo corresponds to the Vashon ice advance into the Puget Lowland between about 18 and 15.3 ka (see discussion and fig. 3 in Polenz and others, 2015). Unit Qgo may include advance outwash lower in the subsurface; the upper part corresponds to the glacial maximum and recession.

Qpog **Pre-Vashon outwash gravel**—Pebble gravel and sand, in most exposures weathered to saprolite or clayey soil with only faint evidence of former pebble content; pale gray; weathers medium to pale

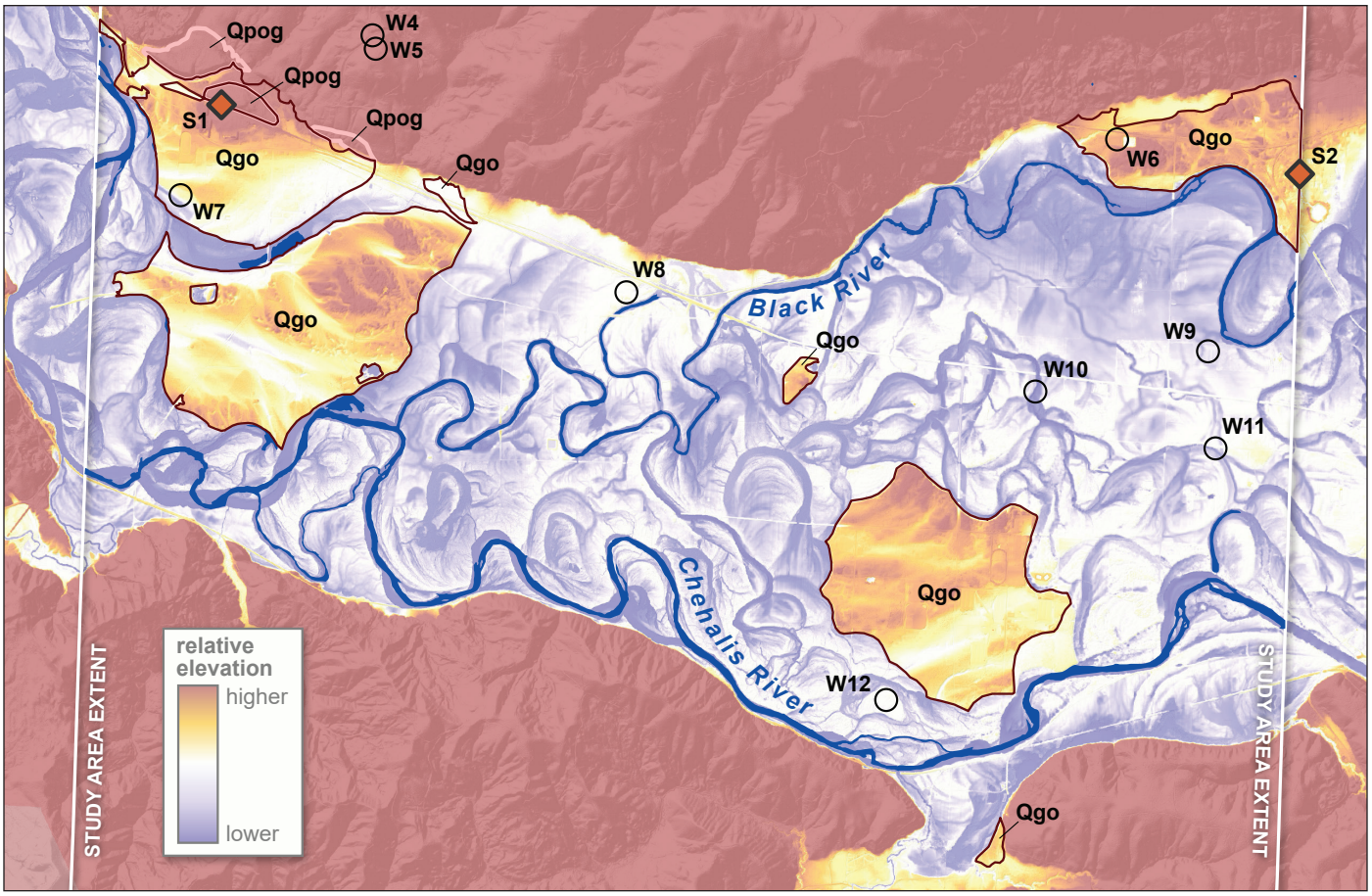

Figure 1. Lidar-based relative elevation model of the Chehalis River valley across the Oakville quadrangle. White lines on both sides mark quadrangle edges. Color ramp shows low elevations (and water) in dark blue and progressively more elevated areas in light blue to pale greenish blue, then yellow and red. Open circles (for example, W9) are water wells shown on the map. Red diamond is an approximate water well location (likely just outside the map area) referenced in the text as significant site S2. Vashon outwash deposits are revealed as elevated (yellow to red) relict terraces (inselbergs) above the surrounding valley floor. Note that these lack the otherwise abundant meander bends of active and relict channels across the combined flood plain of the Chehalis and Black Rivers.

brown, tan and light orange; moderately to strongly weathered in all observed exposures; loose to moderately compact; clasts rounded, sand matrix locally subangular; moderately to well-sorted; lithologically diverse and northern-sourced from the Olympia and Yelm ice lobes, with lithologic trends similar to those in unit Qgo (see *Late Pleistocene continental glacial deposits* above). Unit Qpog is mapped in terraces along the southwestern base of the Black Hills at Oakville based on prior mapping (Logan, 1987; Walsh and others, 1987), the presence of high grade metamorphic clasts that favor northern provenance, weathering, and its elevation above unit Qgo (Fig. 1). Based on well records and drill cuttings east of the map area (Polenz and others, 2018, 2019), the unit is inferred underground in the Chehalis River valley between Gate and Oakville. Together with units Qgo and Qa, unit Qpog forms a highly permeable and productive, generally unconfined aquifer. These traits also render the aquifer sensitive to pollution and the surface prone to drought.

The age of unit Qpog is constrained by clast weathering, which Bretz (1913) noted in pre-Vashon outwash near Oakville (likely near or west of significant site S1) as "somewhat softened on the surface" but "firm within", consistent with our own observations, although we observed more varied weathering across multiple sites. Polenz and others (2017) referred to luminescence age data and weathering in suggesting a Possession drift age (MIS3) for comparably (?) weathered clasts in outwash about 4.5 mi northeast of the map area, in contrast to clearly older drift noted by Polenz and others (2019) 4.3 and 5.9 mi east of the map area. These data suggest that unit Qpog in the subsurface includes deposits from two or more pre-Vashon glaciations that Polenz and others (2019) suggest are likely <1 Ma old.

ALPINE GLACIAL DEPOSITS

Qapolh **Logan Hill Formation (Pleistocene)**—Sandy pebble gravel and sand, deeply weathered in all exposures to clay, fine sand, or silt, except for some quartz clasts; multicolored, red to reddish brown, brown and yellowish brown; strongly

weathered to rotten except for some quartz; mildly to moderately compact, poorly indurated; clasts mostly well-rounded and equant to oblate, with imbrication weakly suggested in some exposures outside the map area (Polenz and others, 2019); matrix rounded to subangular. Observed clasts and sand are mostly quartz. Exposures east of the map area revealed abundant intermediate to felsic igneous rocks and smaller amounts of mafic igneous rocks, metamorphic rocks, and quartz (Polenz and others, 2019; Sadowski and others, 2019). The high quartz content observed in the map area suggests that less resistant lithologies have weathered out of the near-surface exposures here. Unit Qapolh is approximately 50–80 ft thick on Michigan Hill based on well records and slope exposures east of the map area (Polenz and others, 2019). Unit may reach 130 ft thick south of the Doty fault, based on mapped extent, and up to 170 ft thick east thereof (Sadowski and others, 2019). The unit unconformably overlies bedrock. U-Pb analysis of detrital zircons from age site GD85 about 50 ft below the hilltop surface on Michigan Hill yielded an age of <2.9 ±0.6 Ma, consistent with U-Pb ages elsewhere (Polenz and others, 2019; Sadowski and others, 2018, 2019). The Logan Hill Formation has been interpreted as Cascade Range-sourced, alpine glacial outwash (Snavely and others, 1958), and our tentative assessment is that all available U-Pb age spectra are consistent with that provenance. However, the two Michigan Hill samples (age site GD85 of this study and age site GD6 of Polenz and others, 2019) contain few middle Eocene through Miocene zircons, unlike samples farther south (Sadowski and others, 2018, 2019). This suggests that the unit at Michigan Hill has a different mix of sediment sources. It may, for instance, be derived at least partly from a more northern watershed. One sample ~13.5 mi southeast of the map area yielded a <0.84 ±0.38 Ma age (WGS unpublished data, sample 18LH1P), indicating that at least south of the map area, some deposits mapped as this unit are much younger than 2.9 ±0.6 Ma.

Quaternary to Eocene Continental Deposits

QEcf
QEcf$_s$ **Terrestrial weathering clay**—Clay and (or) silt in saprolite or soil developed mostly from basalt of the Crescent Formation (where mapped as unit QEcf) or mostly from siltstone of unit Enf (where mapped as unit QEcf$_s$); locally includes corestones of basalt in QEcf or sedimentary rock in QEcf$_s$; unit QEcf colored mostly orange brown to reddish brown and medium brown, commonly with strongly weathered to rotten corestones of greenish gray to black basalt; unit QEcf$_s$ colored mostly pale yellowish brown to brown, commonly with chips (usually <2 cm) of pale gray or pale yellow siltstone; loose and soft near surface but stiff in some exposures; homogeneous except where saprolite preserves primary structure; >44 percent halloysite and 15–26 percent goethite where basalt based, and >60 percent smectite (nontronite) in sedimentary rock-based facies (based on X-ray diffraction analyses of clays from the unit northeast of the map area, Polenz and others, 2017). We observed 20 ft of unit thickness 400–500 ft southeast of geochemistry site G2; exposures northeast of the map area suggest the unit is commonly >30 ft thick (Polenz and others, 2017). The unit is mapped where it fully conceals bedrock in the Black Hills in the northern portion of the map area; its sedimentary unit QEcf$_s$ was identified near the northeast end of the map area and southwest of U-Pb age site GD81. Unit age for both units is constrained to less than its parent material and thought to be slightly younger for unit QEcf$_s$ because the sedimentary rock exposures we observed seem to onlap and post-date the basalt. Related considerations are further discussed by Polenz and others (2017) in the context of weathered exposures of McIntosh Formation northeast of the map area (in this map, the McIntosh Formation is largely equivalent to unit Enf and its weathering products within unit QEcf$_s$).

Tertiary Volcanic and Sedimentary Bedrock

Mc$_w$ **Wilkes Formation (middle to late Miocene)**—Siltstone, locally overlain by and may be interbedded with basalt-clastic, cobbly pebble conglomerate; white to pale yellow, pale gray, and pale brown, weathers pale yellow with orange to reddish brown iron staining; clasts dark, medium, or pale gray, with thick, reddish brown, orange and gray to greenish gray weathering rinds; soil pale to strong brown and yellowish brown, grayish brown and reddish brown, matrix locally pale gray; poorly lithified; clasts rounded, but where observed, rounding is partly from weathering; well-sorted in siltstone, locally with thin sandstone interbeds; poorly sorted in conglomerate; siltstone planar-bedded and hackly, with strong, bedding-parallel platy partings; 3-ft-thick gravel facies at and near age site GD88 apparently lacks bedding but is concordant with underlying siltstone; siltstone-quartz feldspathic, usually with trace amounts of muscovite and dark opaque minerals; conglomerate facies clasts nearly all porphyritic to aphanitic basalt, but also include a few more felsic igneous or quartzitic rocks. Unit thickness south of the Doty fault is about 630 ft, based on Cross Section A–A′. The unit is likely thinner but is essentially of unconstrained thickness farther north along the western map edge near age site GD88. Unit Mc$_w$ is mapped between the Doty fault and the Chehalis River valley in the south half of the Rainbow Falls quadrangle, and between the north and south forks of Lincoln Creek near the western map edge. The combination of planar-bedded siltstone and gravel

facies within the map area, and abundant carbonized plant matter observed elsewhere (Roberts, 1958; Snavely and others, 1958; Sadowski and others, 2019), suggests that the depositional setting ranged from terrestrial to deltaic or marine. Conglomerate clast lithologies suggest derivation from a mix of lavas exposed in the Doty Hills west of the map area: Crescent Formation and alkaline forearc lavas (AFL—see *Whole Rock Geochemistry Results and Discussion*). The age of the unit is <11.2 ±1.3 Ma at age site GD88 (see Tables DS1A and DS1C), and Sadowski and others (2019) reported ages for the unit just east of the map area including <13.6 ±1.9, <13.4 ±1.0, and <6.2 ±1 Ma, and they correlated the unit to the Wilkes Formation of Roberts (1958) and the nonmarine unit of Snavely and others (1958).

Ꝡvgs **Sentinel Bluffs member of the Grande Ronde Basalt of the Columbia River Basalt Group (middle Miocene)**—Aphanitic, vesicular basaltic andesite; dark to light gray where fresh; yellowish gray, medium brown exteriors where moderately weathered; hard and crystalline; commonly blocky with columnar-jointed colonnade and lesser entablature; sometimes structureless, rarely with platy zones and (or) flow-top breccia, and lacking observed pillows within the map area; contains equant vesicles (<7 mm) and zeolite-filled amygdules. Sentinel Bluffs member basalt in the map area appears to be laterally continuous with exposures east of the map area, where geochemical analyses of major and trace elements have been used to assign tholeiitic, basaltic andesites to the McCoy Canyon(?) flow of the Sentinel Bluffs member of the Grande Ronde Basalt (Reidel, 2005; Sadowski and others, 2019). Less than 180 ft of unit thickness is suggested by outcrop patterns and combined modeling of gravity and aeromagnetic data, except where thrust stacking locally thickens the unit (Cross Section A–A′). Just south of the Doty fault zone, well W33 intersected 102 ft of the unit; north of the southern thrust strand of the fault zone, well W34 intersected 75 ft. The unit was observed south of and between strands of the Doty fault. Whereas observed exposures in the map area are limited to flows that may have been deposited subaerially, subaqueous deposition is suggested west of the map area by weak palagonitic pillows ~6.1 mi west of the map area on the west side of the Doty uplift, and by weak palagonitic pillows and weathered peperitic structures ~9.3 mi west-southwest of the southwest corner of the map. Unit Ꝡvgs is sandwiched by Astoria(?) Formation in the Chehalis River syncline and conformably overlies Astoria(?) Formation farther north and south (Cross Section A–A′). Deposition of unit Ꝡvgs partly baked the underlying Astoria(?) Formation marine sandstone.

Ꝡma **Astoria(?) Formation (early to middle Miocene)**—Marine siltstone and very coarse to very fine grained sandstone; rare pebbles locally observed in soil underlain by the formation; locally includes volcaniclastic conglomerate and detrital carbonized wood (Polenz and others, 2019); pale yellow to pale brown, light gray to olive green, orange and light orange, with red, orange, and brown iron stains; moderately or heavily weathered in all observed exposures, commonly forming pale, dark, or reddish brown or gray soil; mostly poorly lithified; sand fraction rounded to subrounded; particles in soil developed from Astoria(?) Formation less rounded than in nearby exposures of Logan Hill Formation; poorly sorted in siltstone, moderately to well-sorted in sandstone; bedding not directly observed at Michigan Hill, but preferentially oriented mica flakes suggest bedding in some siltstone exposures; Rainbow Falls quadrangle exposures reveal thick to very thick beds, locally with siltstone interbeds and locally with wavy cross-bedding; mostly quartz and feldspar, with a diverse range of less common minerals, some of which are described next. Siltstone contains trace amounts to <1 percent mica and trace amounts of dark opaque minerals. Sandstone contains trace amounts to 2 percent mica, in some exposures including gray mica (lepidolite?) not normally noted in Lincoln Creek Formation or Eocene sedimentary rocks in the map area, and trace amounts to 7 percent dark opaque minerals. Previous workers identified a relative abundance of heavy minerals as a distinguishing feature of the Astoria(?) Formation compared to older sedimentary rocks (Snavely and others, 1958; Polenz and others, 2019). Soils developed from the unit appear to contain a lithologically more diverse sand fraction than soils of nearby Logan Hill Formation exposures.

The Astoria(?) Formation was mapped on Michigan Hill in the Oakville quadrangle, where the mapped extent of the unit suggests about 200 ft of unit thickness. The Astoria(?) Formation at Michigan Hill is overlain by the Logan Hill Formation, and it both rests on and crops out laterally adjacent to the Lincoln Creek Formation. In the Rainbow Falls quadrangle, the Astoria(?) Formation is mapped between strands of the Doty fault, where Astoria(?) Formation is upsection of the Lincoln Creek Formation and downsection of the Columbia River Basalt. Along the lower hillslopes of valleys south of the Doty fault, Astoria(?) Formation rests upsection of the Lincoln Creek Formation, straddles Columbia River Basalt, and is downsection of the Wilkes Formation. Cross section A–A′ suggests more than 800 ft of unit thickness south of the Doty fault. In the Rochester quadrangle east of the map area, Polenz and others (2019) inferred from field relations and age control data that the Astoria(?) and Lincoln Creek Formations may be separated by

an unconformity. They further noted that different zircon spectra suggest these formations are derived, at least partly, from difference sources, and that basaltic pebbles within the Astoria(?) Formation along and east of the eastern edge of the Oakville quadrangle are derived from Middle Eocene volcanic rocks of Grays River of Phillips and others (1989; refer to Polenz and others, 2019, geochemistry sites G30–G38). This finding is now superseded by the discovery of the Doty Hills basalt lavas west of the Rainbow Falls and Oakville quadrangles. The lavas provide a much better chemical match for the basalt clasts in the Astoria Formation at the eastern edge of the Oakville quadrangle and those in the younger Miocene Wilkes Formation on the west side of the Rainbow Falls quadrangle (see *Whole Rock Geochemistry Results and Discussion*). The paleogeographic extent, abundance, and distribution of the Doty Hills basalt remain mostly unknown; inferences about provenance of reworked Doty Hills basalt clasts therefore remain speculative. However, the presence of the chemically similar clasts in both Astoria(?) and Wilkes Formation within the map area suggests that terrestrial sediment from the Doty Hills (west of the map area) contributed to the map area throughout much of the Miocene and at present. The Astoria(?) Formation text references are followed by a question mark because the type section in Oregon (Howe, 1926; Beaulieu, 1971) has been obliterated by development such that correlation to it is no longer testable.

ⓓEmlc **Lincoln Creek Formation (late Eocene to earliest Miocene)**—Marine siltstone and fine-grained sandstone; locally tuffaceous or fossiliferous; pale gray to pale yellowish gray, pale yellow and pale greenish gray, weathers pale yellowish brown and pale orange with common orange to deep red mottled surfaces; moderately to poorly lithified except in well-lithified, commonly fossiliferous calcareous concretions; locally hackly and spheroidally weathered; sandstone grains subangular to subrounded and well-sorted; siltstone mostly lacks bedding; sandstone ranges from not bedded to bedded. Most exposures contain <1 percent each of mica and dark opaque minerals, but dark opaque minerals locally comprise up to 5 percent. A 1,600 ft unit thickness is suggested by a cross section near the eastern map edge beneath Michigan Hill (Polenz and others, 2019), where exposures suggest that the upper 300 ft of section are equivalent to the tuffaceous siltstone facies of Snavely and others' (1958) Lincoln Formation. Outcrop patterns and well records suggest a few hundred foot unit thickness in the southwestern Black Hills north of Oakville. In the vicinity of the Doty fault, we estimate about 850 ft unit thickness (Cross Section A–A'). The Lincoln Creek Formation is exposed in the southwestern Black Hills and on Michigan Hill northeast of the Scammon Creek fault. The unit is also mapped in the south central portion of the Rainbow Falls quadrangle. We suspect that the Lincoln Creek Formation unconformably onlaps Crescent Formation basalt throughout the southwestern Black Hills, as suggested by Beikman and others (1967). The Lincoln Creek Formation is generally older than the Astoria(?) Formation, but at the eastern map edge on Michigan Hill, detrital zircon U-Pb data suggest similar ages for both units—which in this area appear to be partly laterally adjacent and partly separated by an unconformity (Polenz and others, 2019). Fossils indicate a late Eocene age for the base of the formation north of Oakville (Van Winkle, 1918; Weaver and Palmer, 1922; Weaver, 1937, 1943; Armentrout, 1973; unpublished records, Burke Museum of Natural History and Culture, Seattle, WA). A <30.3 ±1.1 Ma U-Pb age on detrital zircons at age site GD82 suggests an early Oligocene age for collocated shallow marine fossils (age site GD5). Pease and Hoover's (1957) assertion that the formation ranges to Miocene age is confirmed by fossils and a <20.3 ±1.7 Ma U-Pb age from the type section near the eastern map edge (Polenz and others, 2019).

En
Enf
Ens

Nearshore, deltaic, and marine turbiditic sedimentary rocks (middle to late Eocene)—Undivided unit En includes micaceous siltstone and sandstone, locally claystone and coal seams; mapped as subunit Enf where mostly siltstone; mapped as subunit Ens where mostly sandstone; sandstone pale olive gray to pale blueish gray and pale brown, and weathering pale yellow, pale yellowish brown, and reddish brown with common orange oxidation banding; olive gray to pale greenish gray, pale olive brown, pale gray, and pale yellow in siltstone and claystone, and weathering tan, yellow, orange, brown, and reddish brown. All textures of the unit are commonly crumbly and friable, hackly, or spheroidally weathered and rarely more than moderately lithified. Sandstone is fine-grained, subrounded to rounded or subangular, and moderately sorted to well-sorted—in most exposures better sorted than the siltstone. All textures of the unit are unbedded to well-bedded with faint, thin, planar or gently undulating beds and laminae commonly expressed only by preferential bedding-parallel mica flakes and (or) fissile partings. Siltstone locally contains interbeds or lenses of medium to coarse grained sandstone with rip-up clasts of the siltstone. All textures of the unit are quartz-feldspathic and commonly tuffaceous. Most exposures of siltstone contain <1 percent each of muscovite mica and dark opaque particles, and most exposures of sandstone contain traces to 3 percent of muscovite mica and traces to 2 percent of dark opaque particles. In both sandstone and siltstone, mica is more abundant than dark opaque particles, and fewer than 6 percent of

the samples revealed a few flakes of golden mica (phlogopite?). Five to 10 percent pale to dark gray particles observed in some sandstone exposures appear to be mostly felsic to intermediate volcanic lithic fragments.

Relief between Oakville and Independence Valley suggests about 600 ft exposed unit thickness, but abundant landslides render bedding orientations and section thickness estimates questionable. Cross Section A–A′ suggests about 4,500 ft unit thickness at the south end and about 3,000 ft at the northeast end of the section—inferred mostly from combined modeling of gravity and magnetic anomalies (partly informed by well records outside the map area).

Unit En is widely exposed on the Lincoln Creek uplift between the Scammon Creek and Doty faults, where siltstone subunit Enf forms most exposures. However, sandstone subunit Ens forms most exposures between the Chehalis River and Independence valleys within the Lincoln Creek uplift. Subunit Ens is also widely mapped between strands of the Doty fault. Snavely and others (1958) identified coal within subunit Ens at and near well W16 just southwest of the Scammon Creek fault as the Tono No. 1 coal bed (low in the Skookumchuck Formation). Siltstone unit Enf appears to onlap Crescent Formation basalt in the southern Black Hills, although no contact relations were observed.

We interpret the undivided unit En as the sedimentary record of a long-lasting Eocene marine delta system such as envisioned by Buckovic (1979) and Sadowski and others (2018), wherein subunit Enf is mostly siltstone of marine origin and subunit Ens is mostly sandstone that ranges from shallow marine deltaic to freshwater settings. Unit En broadly corresponds to deposits mapped by Logan (1987) as McIntosh Formation in the Black Hills east of Oakville and Lincoln Creek Formation north of Oakville, and as Skookumchuck Formation elsewhere in the map area. Except where Lincoln Creek Formation is mapped north of Oakville, the geographic distribution of siltstone (unit Enf) observed in this study largely coincides with Pease and Hoover's (1957) mapping of McIntosh Formation. We mapped sandstone unit Ens largely where Pease and Hoover (1957) and Snavely and others (1958) mapped Skookumchuck Formation. We combined both formations into unit En because we identified no consistently mappable difference in outcrop or chronometric age-control data; the youngest single zircons from nine 'McIntosh Formation' samples range from <47.6 Ma to <39.5 Ma (Polenz and others, 2017, 2018; Sadowski and others, 2019; age sites GD81, 84, 89, 90, and 91 from this study, see Table DS1A) and those in two 'Skookumchuck Formation' samples range from <43.4 Ma to <40.7 Ma (Polenz and others, 2019; age site GD87 from this study). Shell macrofossils are common in unit En. Most are poorly preserved, and fossil samples from this study yielded no biostratigraphic constraints, but a few yielded paleoenvironmental constraints that confirm the depositional settings in unit En ranged from freshwater to marine (Table DS2). Bivalve molds at age site GD40 (subunit Ens, U-Pb age site GD87) and a leaf imprint at age site GD38 (subunit Enf) suggest unit En is correlated with the Cowlitz Formation as mapped southeast of the map area by Henriksen (1956) and Roberts (1958).

Em **Marine sedimentary rocks (Eocene)**—Volcaniclastic lapilli tuff breccias interbedded with basaltic sandstone and siltstone; medium to dark gray and black, weathers light to medium gray, olive, light orange to red, and, uncommonly, white (in matrix clay); moderately compact, moderately to heavily indurated; locally well cemented; sandstone moderately to well-sorted, breccias poorly sorted with faint, medium to very thick planar beds; sandstone beds thin and planar, with meter-scale interbeds of thickly laminated to thinly planar-bedded mudstone and siltstone; clast lithologies exclusively basaltic; sandstone mostly basaltic lithic, with minor plagioclase and unidentified red grains, <1 percent white mica and trace amounts of quartz. The rock is unstructured at outcrop scale, does not resemble other observed exposures, and appears to be submarine resedimented hyaloclastite. Isolated bivalve shell fragments at significant site S3 (sec. 25, T14N R5W, lat. 46.6768, long. -123.2461) confirm a sedimentary depositional setting.

Unit Em is found along the western map edge just north of the Doty fault and may be up to 500 m thick. We interpret unit Em as proximally volcaniclastic based on its overwhelmingly basaltic content of clasts and sand-sized lithic fragments, and the presence of abundant lapilli. The planar bedding in sandstone, siltstone, and mudstone are interpreted as marine. Due to limited exposure in the map area (especially poor where queried west of age site GD91), the unit is described mostly based on observations in the Doty Hills west of the map area, where it rests on Crescent Formation. Crescent basalt exposures in the Doty Hills west of the map area suggest that unit Em is at least partly derived from Crescent basalt. However, geochemical data from a volcanic clast collected from the same(?) unit at geochemistry site G40 (2,200 ft west of the map area, sec. 24, T14N R5W; -123.26001, 46.68662) resembles younger Eocene alkaline forearc lavas (AFL—see *Whole Rock Geochemistry Results and Discussion*), which are exposed beneath sedimentary rocks at the base of the Lincoln Creek Formation on the west side of the Doty Hills. A mix of geochemically similar AFL-derived clasts and Crescent Formation-derived clasts (geochemistry sites G28-G37) is present in the Wilkes Formation pebble conglomerate that rests concordantly on planar-bedded siltstone 3 mi

farther north at age site GD88. This suggests that some sedimentary rocks along the western map edge that resemble—and may include—deposits in unit Em may be younger than recognized from available exposures and field relations. However, based on the limited available exposures, unit Em appears concordant and in sharp contact with the underlying Crescent Formation and conformable (and interfingering?) with overlying Eocene nearshore sedimentary rocks (unit En).

Ev_C **Crescent Formation (early Eocene)**—Plagioclase-pyroxene tholeiitic basalt (previously reported to include local, minor sedimentary interbeds by Pease and Hoover [1957] at age site GD16 [sec. 27, T16N, R4W] and elsewhere in the Black Hills by Logan, 1987); black to dark gray, commonly with greenish tint, weathers grayish green and medium brown to orange; mostly aphanitic but ranging to phaneritic; locally brecciated; poorly to well-developed columns revealed in most quarries are rarely apparent elsewhere and suggest minimum flow thicknesses of 20–60 ft; pervasively chloritically altered; commonly contains amygdules of zeolite, chlorite, calcite, or quartz. The Crescent Formation is exposed mostly along streams in the Black Hills and southwest of the Scammon Creek fault.

Contact relations with downsection and upsection units are mostly unexposed in the map area. The Crescent Formation is part of the Siletzia terrane (Wells and others, 2014; Eddy and others, 2017) and appears to form much of the dense, igneous basement rocks beneath the map area. The sedimentary rocks we observed near Crescent Formation basalt rest on and mostly appear to onlap the basalt, but the contact relations usually are unexposed. A localized exposure of seemingly sheared conglomerate (lapilli tuff?) with basalt clasts and calcite-cemented matrix at geochemistry site G11 is in sharp, planar contact with upsection Lincoln Creek Formation(?) siltstone (geochemistry sample G10); this conglomerate may be part of the Crescent Formation but could also be younger. North of Oakville, fossils, and U-Pb ages from age sites GD82 and GD83, identify onlapping sedimentary rocks as the Lincoln Creek Formation. South of Oakville, and farther east in the Black Hills, sedimentary rocks may be concordant or onlapping and are more commonly tuffaceous than would be typical within the Crescent Formation; U-Pb ages at site GD81 northeast of Oakville and northeast of the map area (Polenz and others, 2017) support association with the McIntosh Formation (here included with unit En), as does U-Pb age site GD84 southwest of Oakville.

Two approximately located paleomagnetic measurement locations in the map area document magnetically reversed Crescent Formation basalt (M1, M3), a third (M2) documents normally magnetized basalt (Globerman, 1981). Radiometric ages constrain the Crescent Formation in the southern Black Hills to between ~55 and 47.4 ±0.2 Ma (Polenz and others, 2017; Eddy and others, 2017, Wells and others, 2014). Ulatisian- or lower Narizian-age fossils from the southern Black Hills are consistent with this age range (Polenz and others, 2017).

WHOLE ROCK GEOCHEMISTRY RESULTS AND DISCUSSION

A total of 46 samples were selected for whole rock major and trace element analysis. Represented within those are 13 Crescent Formation lavas (including two corestones), 11 volcanic clasts from conglomerate beds, and 21 sedimentary rocks that are mainly siltstones and sandstones.

All of the Crescent Formation samples classify as tholeiitic basalts (Fig. 2), display limited chemical variation (for example, 47.5–50.9 wt. % SiO_2, 5.7–7.3 wt. % MgO), and overlap in composition with Crescent lavas analyzed during previous WGS quadrangle mapping projects (Polenz and others, 2012a,b, 2014, 2017; Contreras and others, 2012). In the Littlerock quadrangle (northeast adjacent to the map area), Polenz and others (2017) were able to divide Crescent samples into a more-enriched group and a less-enriched group, a distinction attributed to chemical differences in their mantle source regions. All Crescent Formation samples from this mapping project belong to the more-enriched group, which Polenz and others (2017) associated with the Willapa Hills and Black Hills. This more enriched group is marked by higher contents of TiO_2 and La/Yb(N), and lower contents of Y/Nb and Zr/Nb. The less-enriched lavas from the Littlerock quadrangle instead resemble lavas found on the Olympic Peninsula (Polenz and others, 2017), with lower contents of TiO_2 and La/Yb(N), and higher contents of Y/Nb and Zr/Nb.

The ten volcanic clasts collected from a pebbly conglomerate layer in the Wilkes Formation can be divided into two geochemically distinct groups (Table 1). Group 1 consists of five tholeiitic basalt clasts (geochemistry samples G29, G31, G33, G36, G37) that closely resemble Crescent Formation lavas (Figs. 2 and 3; Table 1) and one tholeiitic andesite clast (geochemistry sample G32) that appears to be a Crescent basalt differentiate. The latter sample is highly enriched in incompatible elements (for example, Zr, Th, Ba) and depleted in compatible elements (for example, Cr, V), consistent with it being the product of extensive fractional crystallization. The four Group 2 clasts in Table 1 (geochemistry samples G28, G30, G34, G35) are alkaline basalts characterized by low SiO_2 contents coupled with high MgO contents and high levels of incompatible elements (for example, Rb, Nb). Another rock of similar composition (geochemistry sample G40) was collected from soil 2.6 mi farther southwest (46.68659°N, -123.26004°W—2,200 ft west of the map area). The Group 2 clasts may be sourced from geochemically similar, scattered, small volume mafic lavas, such as the Pe Ell Volcanics (Henriksen, 1956) that erupted in the Cascadia forearc after the accretion of Siletzia and have been termed alkaline forearc lavas (AFL) by Organ and others (2019) (Fig. 3). In particular, Group 2 clasts are nearly identical in composition to the late Eocene(?) 'Doty Hills basalts' (Table 1), a subset of AFLs sampled from small exposures in the Doty Hills west of the map area (for example,

Table 1. Chemical characteristics of clasts from this mapping project (Groups 1 and 2) compared to potential source rocks. Major oxides in weight percent, trace elements in parts per million. Averages are reported with 1 sigma standard deviation (in parentheses). AFL and Doty Hills data are from Organ (2020); Crescent data compiled from Contreras and others (2012), Polenz and others (2012a,b, 2014, 2017). Note the similarities between Group 1 clasts and Crescent Formation basalts and between Group 2 clasts and the Doty Hills basalts. See Table DS1A for more details.

	Group 1 Clasts (n=5)	Avg. Crescent (n=42)	Group 2 Clasts (n=5)	Avg. AFL (n=12)	Avg. Doty Hills (n=6)
SiO_2	48.0–49.2	48.3 (1.2)	46.0–46.4	48.8 (3.5)	45.6 (0.7)
TiO_2	2.6–2.8	2.3 (0.5)	3.1–4.2	2.5 (0.7)	3.2 (0.4)
MgO	5.0–6.0	6.7 (0.7)	5.1–10.6	5.9 (3.3)	8.6 (2.4)
Nb	16–18	13 (4)	52–53	43 (11)	52 (29)
Rb	2–8	3 (2)	14–25	14 (11)	20 (0.7)
La/Yb	2.6–3.6	3 (0.6)	9.1–12.1	8.4 (0.6)	12.2 (5.3)
Sr/Y	4–5	9 (4)	18–23	13 (3)	40 (13)

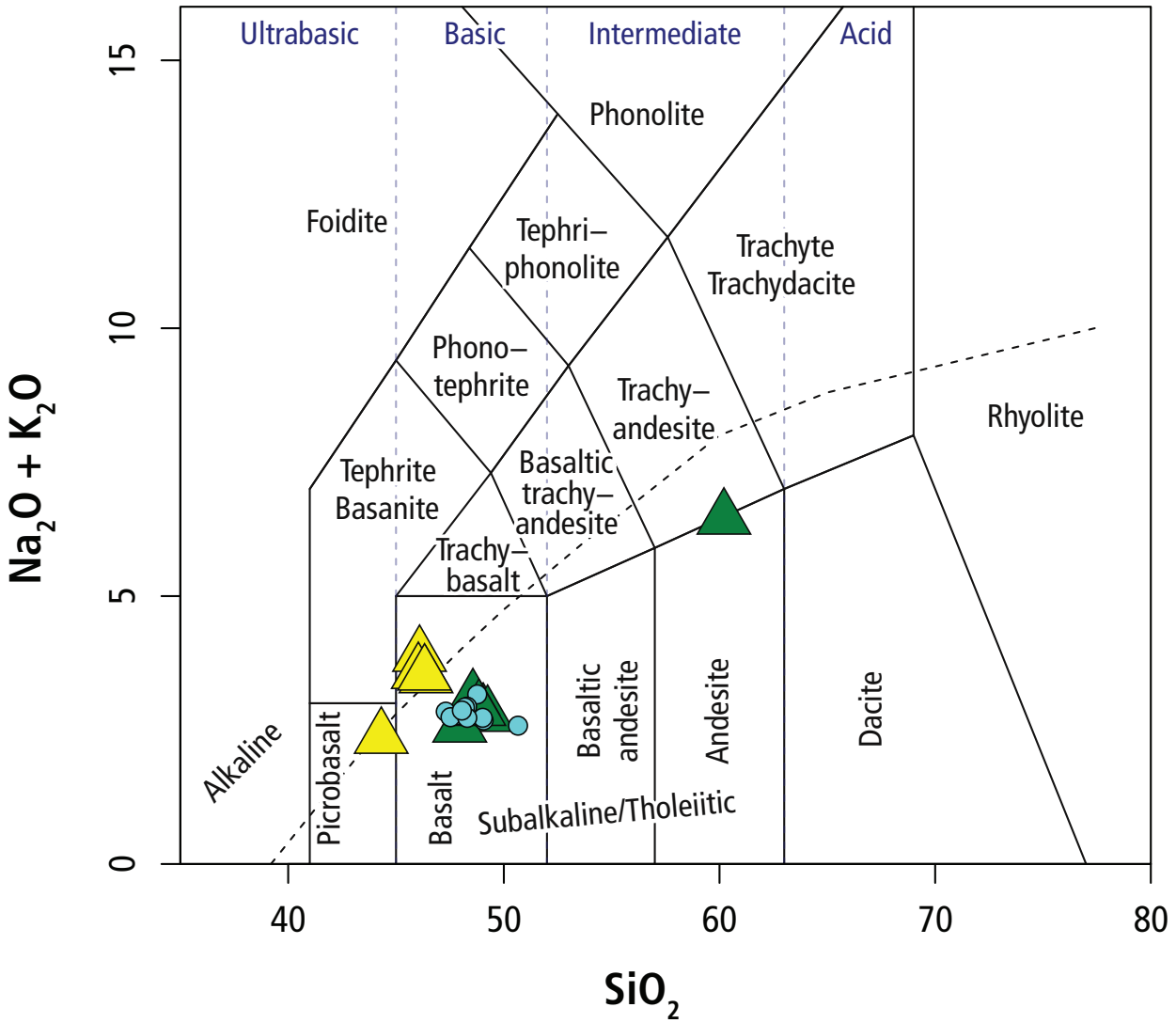

Figure 2. Total alkalis vs. SiO_2 volcanic classification plot (Le Bas and others, 1986). Known Crescent Formation samples are shown as blue circles. Group 1 clasts (green triangles) and Group 2 clasts (yellow triangles) are detrital clasts sampled from the Wilkes Formation. Note the overlap between Crescent samples and Group 1 clasts and the alkaline nature of Group 2 clasts.

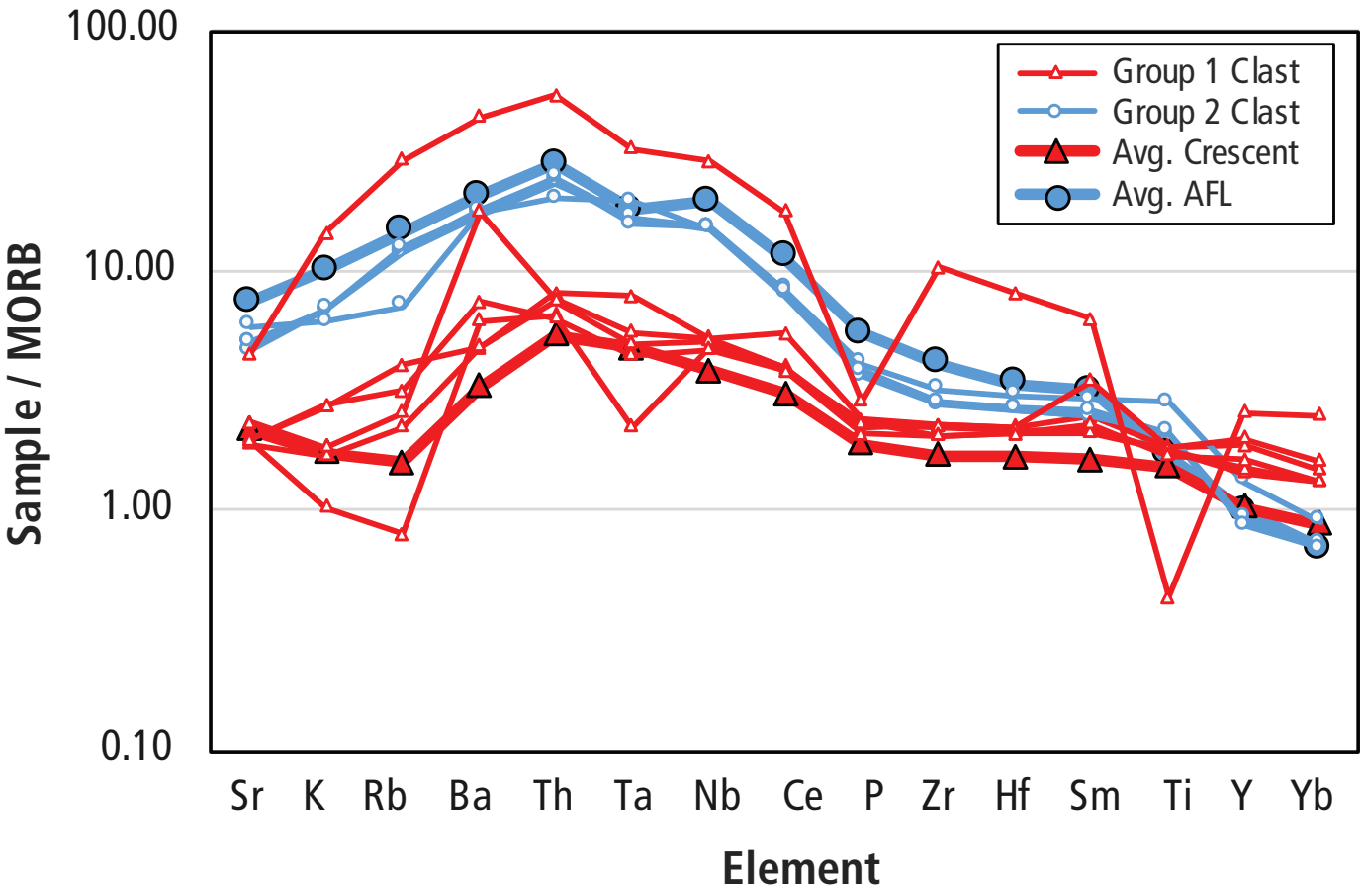

Figure 3. MORB-normalized spidergram (Sun and McDonough, 1989) illustrating similarities between Group 1 clasts and Crescent Formation basalts, and between Group 2 clasts and AFL samples. The Group 1 clast with highest concentrations of most elements is the andesite (G32), which shows depletions in P and Ti resulting from apatite and Fe-Ti oxide fractionation. Average Crescent and AFL data from sources listed in Table 1.

WGS unpublished data from field site CB-534 at SW1/4, sec. 26, T15N R6W, 46.762634, -123.401669). The La/Yb (N) ratios >10 in the Group 2 and Doty Hills samples indicate these rocks were derived from a garnet bearing mantle source region, a deeper mantle source than the Crescent basalts, whereas the elevated Sr/Y ratios in the same samples suggest they formed from magmas that had undergone little if any feldspar fractionation; in this context, scattered values for Sr/Y are unsurprising. However, the geographic extent of the Doty Hills basalt outcrops (or the broader umbrella category of AFLs) is not well known and it is therefore not possible at present to conclusively attribute clasts from the map area to a specific source area. Additional clasts with the distinctive geochemical traits of Group 2 have been reported in the Astoria(?) Formation along the eastern map edge, where Polenz and others (2019) speculated about possible derivation from volcanics of Grays River (see Polenz and others, 2019, geochemistry samples G30–G38). However, Polenz and others (2019) did not know of the chemically more similar Doty Hills basalt and its outcrops west of the map area.

Available sedimentary rock geochemistry did not yield data that would have helped with unit characterizations.

DESCRIPTION OF STRUCTURES

Discrete domains of geophysical anomalies and topographic scarps and lineaments suggest that the map area straddles several structural domains. Uplift of Eocene Crescent Formation basalt and underlying mafic igneous basement rocks clearly separate the Black Hills north of the Rochester fault and the Lincoln Creek uplift between the Scammon Creek and Doty faults from adjacent basins. The Black Hills and Lincoln Creek uplifts (BH and LCU in Fig. M1) are geophysically expressed by gravity highs due to near-surface Crescent basalt and underlying dense (peridotitic?) basement. Gravity lows in the adjacent basins (Fig. M1) result from low-density sediments above the basalt (Cross Section A–A′).

Apparent onlapping of younger Eocene sedimentary rocks onto older Eocene volcanic rocks (Pease and Hoover, 1957) implies Eocene paleo-topography that suggests the uplifted blocks and basins formed at least partly during the Eocene. Deformation of Eocene and younger sedimentary rocks implies additional, more recent activity. We interpret the structures in the map area as potentially active in the context of Miocene–present, north–south compression within the forearc of the seismically active Cascadia subduction zone (Johnson and others, 2004; McCaffrey and others, 2013; Wells and McCaffrey, 2013), consistent with recent mapping nearby (Polenz

and others, 2017, 2018, 2019; Sadowski and others, 2018, 2019; Anderson and others, 2018, 2019). This north–south compression is also apparent both from long-term paleomagnetic rotations and ongoing crustal motions inferred from GPS measurements. Recorded seismicity is minimal beneath the map area, and the mapped structures have so far yielded no documented post-glacial record of activity.

The Scammon Creek fault marks the southwestern edge of the Rochester basin (Fig. M1). In, and especially east, southeast, and north of this basin, Polenz and others (2018) presented (in their fig. M2) a zone of linear, northwest-trending aeromagnetic anomalies that parallel and in some cases coincide with topographic lineaments also noted by Sadowski and others (2018, 2019). Several northwest-striking faults are aligned with these anomalies and lineaments east of the Rainbow Falls–Oakville map area (Snavely and others, 1958, Polenz and others, 2018, 2019; Sadowski and others 2018, 2019). Farther north in the Puget Lowland, detailed study of a comparable zone of linear, northwest-trending aeromagnetic anomalies and topographic lineaments led Sherrod and others (2008) to recognize a broad zone of deformation riddled with fault strands. This suggests unmapped northwest-striking faults northeast of the Scammon Creek fault in and near the map area. A queried fault of uncertain origin in the Black Hills near the northeast corner of the map is aligned with this fabric and may be best interpreted in that context.

Near the northwest map corner at the northern Oakville trough (see "NOT" label in Fig. M1) and northeast of and east of the trough, strong, southwest-trending, southeast-side-up scarps and lineaments and moderate but systematic, similarly oriented aeromagnetic lineaments (in filtered magnetic data not shown in this publication) suggest basalt flow surfaces, or maybe unmapped structures. A south-southeast-striking fault mapped by Pease and Hoover (1957) at the eastern edge of the northern Oakville trough intersects this fabric; we modified this fault to better align it with landforms and lithologic contacts that each suggest multiple strands. The postulated fault helps explain a gravity low and trough in the basalt surface west of the fault ("NOT" label in Fig. M1), where more than 300-ft-thick Lincoln Creek Formation sedimentary rocks rest on the basalt. The fault is queried because without faulting, Eocene fluvial incision into Crescent basalt might carve a valley. But the several-hundred-foot basin depth and localized extent of the trough favor fault offset or folding. Modeling of gravity and magnetic data rules out east-dipping reverse or thrust offset and suggests west-side-down offset and a west-dipping or vertical fault surface. A tear in the hanging wall of the Rochester fault might have triggered such faulting. The sedimentary rocks may conceal the fault, and offset would likely have commenced, and may have ended, before or during their deposition.

The Lincoln Creek uplift has been defined mainly east of the map area (Snavely and others, 1958; Lasmanis and Hall, 1985; Sadowski and others, 2019) but also appears to extend west of the map area into the Doty Hills (Anderson and others, 2018). A distinct gravity high between the Scammon Creek and Doty faults could not be geophysically modeled without shallow mafic igneous bedrock within this uplift (Fig. M1; Cross Section A–A′). Simultaneous modeling of gravity and aeromagnetic anomalies along the geophysical model lines in Figure M1 further reveals that some of the basalt is reversely magnetized. Globerman (1981) confirmed the existence of reversely magnetized basalt in Crescent Formation at site M3 near the north end of the Lincoln Creek uplift and a mix of normally and reversely magnetized measurements farther north in the Black Hills.

Within about 3 mi southwest of the Scammon Creek fault, streams, scarps, and lineaments are oriented mostly parallel or perpendicular to the Scammon Creek fault. West thereof, the emergence of east-trending lineaments, scarps and streams, Miocene sedimentary rocks near the western map edge, and greater relief in the Doty Hills farther west suggest a distinct domain. However, gravity and aeromagnetic data do not reveal a clear structural boundary across this part of the Lincoln Creek uplift.

The southern half of the Rainbow Falls quadrangle is marked by the exposure of mostly Miocene sedimentary rocks and Columbia River Basalt within the Chehalis River syncline, internally offset and sharply separated from the Lincoln Creek uplift by the east-striking, north-side-up Doty fault zone.

Abundant landslides and thick soils in the map area very likely reduced recognition of structures, especially folds. This is particularly problematic in the Eocene sedimentary rock exposures within the Lincoln Creek uplift, where we suspect that some structural data are compromised by unrecognized landslide activity. We analyzed structural trends in this area in three ways: based on the displayed measurements, a more selective subset of our most trusted measurements, and a more expansive set that additionally includes data not shown on the published map but included in the corresponding GIS data. None of these reviews led to clear structural trends north of the Doty fault. This suggests that many structural measurements that appeared credible in the field are compromised. The mapped structures are consequently based mostly on stratigraphic offsets inferred from biostratigraphic records and (or) chronometric age control, regional structural trends, outcrop distributions, and interpretations of geophysical data. Named structures are discussed below.

Named Faults

ROCHESTER FAULT

The existence of the concealed Rochester fault along the southern edge of the Black Hills is supported by steep potential field gradients with gravity and aeromagnetic highs to the north (Bromery, 1962; Washington Public Power Supply System, 1974; “Southern Black Hills fault” in Lau and others, 2018). An east-northeast-trending, steep gravity gradient (RF in Fig. M1) marks the boundary between high gravity in the Black Hills uplift and low gravity in the Rochester basin. We believe that Polenz and others’ (2019) conclusion east of the map area—that this contrast requires basaltic bedrock south of the Black Hills to drop to a greater depth beneath the Chehalis River valley than can be explained by erosion—similarly applies to the map area. Combined modeling of gravity and aeromagnetic potential field data suggests a gently north-dipping fault plane with about 1 km of north-side-up slip. This is consistent with ongoing north–south shortening (Johnson and others, 2004; McCaffrey and others, 2013). Fault offset also explains exposures of middle to late Eocene sedimentary rocks of unit Enf in the Black Hills north

of the fault, in contrast to Oligocene and younger deposits on Michigan Hill south of the fault, consistent with the findings of Polenz and others (2019) east of the map area.

SCAMMON CREEK FAULT

The southeast-striking Scammon Creek fault (Snavely and others, 1958) crosses the map area from Oakville to the southeast corner of the Oakville quadrangle. The fault alignment shown is a synthesis of field observations southeast of Independence Creek, interpretations of gravity and magnetic potential fields along the full mapped length, and combined modeling of gravity and magnetic anomalies across the southeastern map edge and the Chehalis River valley. Exposure of Eocene rocks southwest of the fault and younger rocks northeast of it suggests relative southwest-side-up offset. Reverse offset on a 75 degree southwest-dipping fault plane was documented in a trench, the location of which we could only approximately determine on the hill south of the Chehalis River crossing (Fig. M1). From this trench, Washington Public Power Supply System (1974) concluded that the fault has not ruptured the trench site in at least 83,000 years. Polenz and others (2019) suggested that the fault may bifurcate near the eastern map edge, based on a split into two gravity gradients near a left step of the fault just east of the map area, consistent with transpression. Analysis of gravity and magnetic anomalies in the map area suggests that the queried strands southwest of the main strand have minor vertical offset. They are supported, however, by a faint, northwest-trending fabric of scarps and lineaments, field-observed changes in bedding dips across some strands, and slightly higher contents of dark, opaque minerals and less muscovite northeast of some strands. They may be evidence of a flower structure or conjugate faults with normal offset that accommodate extension in a hanging wall anticline.

DOTY FAULT

The Doty fault zone is an east-striking cluster of interconnected fault strands stretching from the Doty Hills across the map area (Pease and Hoover, 1957; Snavely and others, 1958; Sadowski and others, 2018, 2019). Anderson and others (2019) estimated a fault length ≥25 mi, and more recent mapping estimated a length of about 48 mi (WGS unpublished data). Two previously mapped strands cross the south half of the Rainbow Falls quadrangle; a newly mapped third strand farther south is discussed below. Cross Section A–A′ indicates kilometer-scale, north-side-up slip across the fault zone. The geometry of the strands is constrained by a synthesis of attitude measurements, potential field geophysics modeling, and truncation of bedrock units. Among these, the well-expressed (ridge-forming) Grande Ronde Basalt (unit Mvgs) is best suited for assessing deformation. At the surface, the northern strand juxtaposes north-striking Eocene siltstone of unit Enf against east-striking (south dipping) Eocene sandstone of unit Ens. About 1.75 mi west of Cross Section A–A′, this strand is truncated by a northeast-striking cross fault. The second strand, about 1 mi south of the northern strand, is well defined by juxtaposition of older Eocene sedimentary rocks on the north side against Miocene sediments on the south side of the fault. This strand is further constrained by abrupt termination of folded Grande Ronde Basalt in three locations: twice where the basalt north of the fault strand is folded into a southeast plunging syncline, and once near the western map edge, where the fault offsets overturned basalt on the south side of the fault. West of there, Pease and Hoover (1957) mapped the Doty fault as a single strand to its terminus at the western margin of the Doty uplift, 5.5 mi west of the map area.

Both fault strands described above are understood to be steeply north dipping (50–80°), north-side-up, oblique-slip reverse faults. Their dip range resembles the 45–70 degree north dip range von Dassow and others (2019) reported for the entire Doty fault zone, and it is constrained by contact relationships, geophysical modeling of gravity and magnetic potential-field data, and observations of subsidiary fault and fracture planes interpreted to be part of the fault zone. Gravity and magnetic potential-field modeling has produced similar results in three cross sections along the Doty fault zone (Cross Section A–A′, and model lines A, C, and E in Fig. M1; Anderson and others, 2019; Sadowski and others, 2019; Reedy and others, 2019). Gravity and magnetic potential-field modeling along cross-section A–A′ also required a small amount of dense, magnetic rock (the only realistic candidate is volcanic rock) in the shallow subsurface at the northern strand of the Doty fault, which led to the inference of a small, queried blind, south-dipping fault within the hanging wall there. Surface observations constraining the fault trace and stratigraphic offsets are consistent with a steep, north-dipping reverse fault. Grande Ronde Basalt in the footwall south of the Doty fault near the western map edge is overturned, consistent with a north-dipping reverse fault. Folding of the Grande Ronde Basalt into a southeast-plunging syncline indicates northeast–southwest compression and (or) rotation of the fault bounded block between Doty fault strands in T14N at Cross Section A–A′ which, paired with observations of fault slickensides elsewhere, indicates a moderate, lateral component of motion on the Doty fault zone. We interpret this component as left-lateral based on the conclusion that the Doty fault zone is kinematically linked to the north-striking, east-side-up Fall River fault that extends north from the western terminus of the Doty fault zone (Anderson and others, 2019; Reedy and others, 2019).

A newly mapped fault that we tentatively interpet as part of the Doty fault zone strikes east-northeast across Grande Ronde Basalt from the southwestern map corner to the Chehalis River. The surface trace of this fault is constrained by deflections of channels along a shallowly dipping slope within the Grande Ronde Basalt, and a small scarp-like ridge along that slope. Electrical resistivity data collected across the structure within the Rainbow Falls quadrangle is consistent with gently north dipping, north-side-up displacement of a high resistivity body (Grande Ronde Basalt) over a low resistivity unit (Astoria(?) Formation sandstone). The fault was first identified from gravity and magnetic potential-field modeling west of the Rainbow Falls quadrangle (Anderson and others, 2019) and is confirmed in gravity and magnetic potential-field modeling along Cross Section A–A′. These models indicate a shallowly north dipping thrust fault that may dip as gently as 10 degrees. Thus this fault projects north into the Doty fault and is therefore tentatively interpreted as part of the Doty fault zone. The surface expression of the fault diminishes to the east where it projects into the Chehalis River valley. A poorly constrained eastern terminus of this fault

is inferred near the Chehalis River because the structure is not observed farther east.

Named Folds

CENTRALIA SYNCLINE

The southeast-trending Centralia syncline of Snavely and others (1958) is broadly expressed as the fault-bounded, downthrown Rochester basin east of the Scammon Creek fault (Fig. M1). A gravity trough (Fig. M1) and the spatial distribution of map units define the basin, with younger units in the basin flanked by Eocene rocks outside the basin. Bedding data within the basin locally suggest the Centralia syncline as an asymmetric fold near the eastern map edge (modified from Snavely and others, 1958)—a relatively small feature within the broader, southeast-deepening Rochester basin.

CHEHALIS RIVER SYNCLINE

The east–west trending Chehalis River syncline runs along and likely controls the morphology of the upper Chehalis River valley. The syncline is asymmetric, with a gently to steeply dipping and locally overturned northern limb that is truncated by the Doty fault.

The hinge of the structure is constrained to the north side of the valley, where it is expressed in gently dipping Miocene sediments of the Wilkes and Astoria(?) Formations, which form a bench along the upper Chehalis River valley margin.

The southern limb of the Chehalis River syncline is revealed by a broad, shallowly north-dipping panel of Grande Ronde Basalt (unit Mvgs) that approximates a dip-panel, dipping generally 10–20 degrees north. South of this, gently to moderately dipping, progressively older stratigraphy is exposed, leading to the crest of the Willapa Hills which exposes Crescent basalt (Wells and Sawlan, 2014).

Unnamed Structures

- A queried, east striking fault 2 mi north of the Doty fault was extended from the adjacent Adna quadrangle into the map area based mainly on a south-side-down gravity trough that terminates 2,000–4,000 ft west of the map edge.
- Crescent basalt exposure southwest of the Scammon Creek fault is interpreted as evidence of a hanging wall anticline.
- A syncline in the Black Hills north of Oakville is retained from Pease and Hoover (1957) because it is consistent with nearby spatial bedrock unit distribution, a local gravity trough, and Lincoln Creek Formation bedding orientation data; a northwestern extension of the syncline that Pease and Hoover showed beyond the map area is omitted because none of the above data extend there; a possible relationship to the older(?) south-striking fault east of it remains unresolved.

SUGGESTIONS FOR FURTHER STUDY

- **Post-Eocene sedimentary rocks along and near the western map edge**—Post-Eocene sedimentary rocks are identified at Miocene age site GD88 but may also extend farther south, and north to age site GD86, where a small population of zircons yielded an inconclusive age. Focused mapping of post-Eocene sedimentary rocks near the western map edge may improve understanding of the history, tectonic development, and internal structure of the Lincoln Creek uplift and would contribute to understanding the tectonics of southwest Washington.
- **Sediment sources and age of unit** Em—Unit Em is more indurated and basalt lithic-rich than other Eocene sedimentary rocks in the map area. Analyses of the chemistry (and ages?) of rocks within the unit could improve assessment of its age and provenance.
- **Timing of Black Hills faulting**—At geochemistry site G8 (sec. 22, T16N R4W), columnar basalt hosts a 12-cm-wide gap oriented 315/88 and filled with banded veins and siltstone matrix with basalt breccia(?), consistent with sigma 3 extension relative to a collocated fault. The vein banding suggests episodic vein growth. Age analysis of the vein material might date fault activity in this part of the Black Hills, where timing of fault activity is mostly unconstrained.
- **Origin of scarps in the Black Hills**—Sharp, straight, mostly north to northeast-trending scarps are visible in lidar and in the field at the southern edge of the Black Hills (secs. 28, 29, and 33, T16N R4W). Some resemble joint orientations and cross both ridges and drainages. No similar features have been noted elsewhere in the Black Hills. The origin of these scarps merits investigation.

Structural Attitudes in the Lincoln Creek Uplift

The Lincoln Creek uplift within the map area disrupts what appears to be a regionally contiguous northwest-trending fold farther northwest and southeast. West of the map area, dips are systematically east-down. Somewhere in the western part of the map area, that seems to end and sedimentary rock exposures go from Miocene at the western map edge to Eocene farther east, north, and south; currently available aeromagnetic and gravity data reveal no clear boundary for interpreting this. We measured bedding, joints, and shears in the Lincoln Creek uplift and these data yielded no clear patterns of deformation, though some were probably influenced by unrecognized landslide effects. All this points to one or more unresolved structural conditions, and recognition of structurally coherent trends would likely be of some regional significance. A systematic effort to measure structural orientations in stream channels, including measurement of undisturbed bedding, joints, and shears, might yet improve structural insights.

ACKNOWLEDGMENTS

We thank: Ruth Martin for microfossil analysis and assistance with fossil sample collection; Colleen Harma and Kirsten Sutter (Confederated Tribes of the Chehalis Reservation) and Kevin Hansen (Thurston County) for assistance with accurately locating selected water wells; Tim Walsh, Pat Pringle, and Josh Logan (all WGS retired) for fielding questions about prior mapping

and other issues; Andrew Sadowski (WGS) for assistance with field work and thoughtful reviews; all other WGS active staff for their edits and guidance; Paul Bakke (USFWS retired) for paleo-hydrologic fluvial-geomorphic considerations; Robin Thomas for assistance with field work; Weyerhaeuser, Port Blakely Tree Farms, Green Diamond, and countless other landowners for land access, local knowledge, historical context, well records, and other information.

REFERENCES

Anderson, Megan; Lau, Todd; von Dassow, Wesley; Reedy, Tabor; Sadowski, Andrew; Horst, Alison; Lockett, Alex; Becerra, Rebeca; Toth, Conner; Steely, Alex; Polenz, Michael, 2019, The Doty fault: What is its place in modern crustal deformation of southwest Washington? [abstract]: American Geophysical Union Fall Meeting, Abstract T33D-0404.

Anderson, Megan; Lau, Todd; von Dassow, Wes; Reedy, Tabor; Staisch, Lydia; Cakir, Recep; Sadowski, Andrew; Polenz, Michael; Becerra, Rebeca; Toth, Conner; Steely, Alex; Walsh, Tim; Norman, Dave; Sherrod, Brian, 2018, The Doty fault network: 3D regional deformation applied to seismic hazard characterization in the forearc of Washington State [abstract]: American Geophysical Union Fall Meeting, Abstract T13I-0356.

Anderson, Tom, 2002, Correction of common lead in U-Pb analyses that do not report ^{204}Pb: Chemical Geology, v. 192, issue 1-2, p. 59–79. [https://doi.org/10.1016/S0009-2541(02)00195-X]

Armentrout, J. M., 1973, Molluscan biostratigraphy and paleontology of the Lincoln Creek Formation (late Eocene-Oligocene), southwestern Washington: University of Washington Doctor of Philosophy thesis, 479 p., 1 plate.

Beaulieu, J. D., 1971, Geologic formations of western Oregon (west of longitude 121° 30′): State of Oregon Department of Geology and Mineral Industries Bulletin 70, 72 p. [http://www.oregongeology.org/pubs/B/B-070.pdf]

Beck, M. E., Jr., 1984, Has the Washington–Oregon Coast Range moved northward?: Geology, v. 12, no. 12, p. 737–740. [https://doi.org/10.1130/0091-7613(1984)12<737:HTWCRM>2.0.CO;2]

Beikman, H. M.; Rau, W. W.; Wagner, H. C., 1967, The Lincoln Creek Formation, Grays Harbor basin, southwestern Washington: U.S. Geological Survey Bulletin 1244-I, 14 p. [http://pubs.er.usgs.gov/publication/b1244I]

Blakely, R. J.; Sherrod, B. L.; Weaver, C. S., 2020, High-resolution aeromagnetic survey of the Centralia area, southwest Washington: U.S. Geological Survey data release. [https://doi.org/10.5066/P9T4UC6W]

Booth, D. B., 1994, Glaciofluvial infilling and scour of the Puget Lowland, Washington, during ice-sheet glaciation: Geology, v. 22, no. 8, p. 695–698. [https://doi.org/10.1130/0091-7613(1994)022<0695:GIASOT>2.3.CO;2]

Booth, D. B.; Troost, K. G.; Clague, J. J.; Waitt, R. B., 2004, The Cordilleran ice sheet. *In* Gillespie, A. R.; Porter, S. C.; Atwater, B. F., editors, The Quaternary period in the United States: Elsevier, p. 17-43.

Bretz, J. H., 1911, The terminal moraine of the Puget Sound glacier: Journal of Geology, v. 19, no. 2, p. 161–174. [https://doi.org/10.1086/621826]

Bretz, J. H., 1913, Glaciation of the Puget Sound region: Washington Geological Survey Bulletin 8, 244 p., 3 plates. [http://www.dnr.wa.gov/publications/ger_b8_glaciation_pugetsound.pdf]

Bromery, R. W., 1962, Aeromagnetic and gravimetric interpretation of the geology of the Malone, Rochester, Pe Ell, and Adna quadrangles, Pacific, Lewis, Grays Harbor, and Thurston Counties, Washington: American University Master of Science thesis, 44 p., 4 plates.

Buckovic, W. A., 1979, The Eocene deltaic system of west-central Washington. *In* Armentrout, J. M.; Cole, M. R.; Ter Best, Harry, Jr., editors, Cenozoic paleogeography of the western United States: Society of Economic Paleontologists and Mineralogists Pacific Section, Pacific Coast Paleogeography Symposium 3, p. 147–163.

Contreras, T. A.; Spangler, Eleanor; Fusso, L. A.; Reioux, D. A.; Legorreta Paulín, Gabriel; Pringle, P. T.; Carson, R. J.; Lindstrum, E. F.; Clark, K. P.; Tepper, J. H.; Pileggi, Domenico; Mahan, S. A., 2012, Geologic map of the Eldon 7.5-minute quadrangle, Jefferson, Kitsap, and Mason Counties, Washington: Washington Division of Geology and Earth Resources Map Series 2012-03, 1 sheet, scale 1:24,000, with 60 p. text. [http://www.dnr.wa.gov/Publications/ger_ms2012-03_geol_map_eldon_24k.zip]

Eddy, M. P.; Bowring, S. A.; Umhoefer, P. J.; Miller, R. B.; McLean, N. M.; Donaghy, E. E., 2016, High-resolution temporal and stratigraphic record of Siletzia's accretion and triple junction migration from nonmarine sedimentary basins in central and western Washington: Geological Society of America Bulletin, v. 128, no. 3–4, p. 425–441. [https://doi.org/10.1130/B31335.1]

Eddy, M. P.; Clark, K. P.; Polenz, Michael, 2017, Age and volcanic stratigraphy of the Eocene Siletzia oceanic plateau in Washington and on Vancouver Island: Lithosphere, v. 9, no. 4, p. 652–664. [https://doi.org/10.1130/L650.1]

Globerman, B. R., 1981, Geology, petrology, and paleomagnetism of Eocene basalts from the Black Hills, Washington coast range: Western Washington University Master of Science thesis, 373 p., 1 plate.

Henriksen, D. A., 1956, Eocene stratigraphy of the lower Cowlitz River-eastern Willapa Hills area, southwestern Washington: Washington Division of Mines and Geology Bulletin 43, 122 p. [http://www.dnr.wa.gov/publications/ger_b43_eocene_stratigraphy.pdf]

Howe, H. V., 1926, Astoria, mid-Tertic type of Pacific coast: The Pan-American Geologist, v. 45, no. 4, p. 295–306.

Jackson, S. E.; Pearson, N. J.; Griffin, W. L.; Belousava, E. A., 2004, The application of laser ablation-inductively coupled plasma-mass spectrometery to in situ U-Pb zircon geochronology, Chemical Geology, v. 211, p. 47–69. [https://doi.org/10.1016/j.chemgeo.2004.06.017]

Johnson, S. Y.; Blakely, R. J.; Stephenson, W. J.; Dadisman, S. V.; Fisher, M. A., 2004, Active shortening of the Cascadia forearc and implications for seismic hazards of the Puget Lowland: Tectonics, v. 23, no. 1, 27 p. [https://doi.org/10.1029/2003TC001507]

Lasmanis, Raymond; Hall, T. L., 1985, A geologic feasibility study for the Superconducting Super Collider: Washington Division of Geology and Earth Resources Open File Report 85-3, 41 p., 6 plates. [http://www.dnr.wa.gov/Publications/ger_ofr85-3_superconducting_super_collider.pdf]

Lau, Todd; Anderson, Megan; Polenz, Michael; Sadowski, Andrew; Becerra, Rebeca; Toth, Conner, Cakir, Recep; von Dassow, Wesley; Reedy, Tabor, 2018, Integrated geophysical investigation and 3D fault characterization of the Rochester and Adna 7.5-minute quadrangles, Thurston and Lewis Counties, Washington [abstract]: American Geophysical Union Fall Meeting, Abstract T13I-0355.

Lea, P. D., 1984, Pleistocene glaciation at the southern margin of the Puget lobe, western Washington: University of Washington Master of Science thesis, 96 p., 3 plates.

Le Bas, M. J.; Le Maitre, R. W.; Streckeisen, Albert; Zanettin, Bruno., 1986, A chemical classification of volcanic rocks based on the total alkali silica diagram: Journal of Petrology, v. 27, no. 3, p. 745–750. [https://doi.org/10.1093/petrology/27.3.745]

Lewis, J. C.; Unruh, J. R.; Twiss, R. J., 2003, Seismogenic strain and motion of the Oregon coast block: Geology, v. 31, no. 2, p. 183–186. [https://doi.org/10.1130/0091-7613(2003)031<0183:SSAMOT>2.0.CO;2]

Logan, R. L., compiler, 1987, Geologic map of the Chehalis River and Westport quadrangles, Washington: Washington Division of Geology and Earth Resources Open File Report 87-8, 16 p., 1 plate, scale 1:100,000. [http://www.dnr.wa.gov/Publications/ger_ofr87-8_geol_map_chehalisriver_westport_100k.zip]

Ludwig, K. R., 2003, User's manual for Isoplot 3.00. A geochronological toolkit for Microsoft Excel: Berkely Geochronology Center, Special Publication no. 4a, Berkeley, California.

McCaffrey, Robert; King, R. W.; Payne, S. J.; Lancaster, Matthew, 2013, Active tectonics of northwestern U. S. inferred from GPS-derived surface velocities: Journal of Geophysical Research Solid Earth, v. 118, no. 2, p. 709–723. [https://doi.org/10.1029/2012JB009473]

Morrison, R. B., 1991, Introduction. *In* Morrison, R. B., editor, Quaternary nonglacial geology—Conterminous U.S.: Geological Society of America DNAG Geology of North America, v. K-2, p. 1-12.

Noble, J. B.; Wallace, E. F., 1966, Geology and ground-water resources of Thurston County, Washington; Volume 2: Washington Division of Water Resources Water-Supply Bulletin 10, v. 2, 141 p., 5 plates. [http://www.ecy.wa.gov/programs/eap/wsb/wsb_All.html]

Organ, R. J., 2020, Diverse Eocene magmatism in the Cascadia Forearc: Petrology of the Hatchet Mountain and Alkaline Forearc Lavas, Southwest Washington: University of Puget Sound Bachelor of Science thesis, 55 p.

Organ, R. J.; Tepper, J. H.; von Dassow, Wesley; Reedy, Tabor, 2019, Petrologic diversity among early Cascade arc lavas in SW Washington state [abstract]: American Geophysical Union Fall Meeting, Abstract T23G09.

Parker, B. L.; Goldstein, B. S.; Futornick, Z. O.; Pringle, P. T., 2008, Sedimentological evidence for an enriched glacial outburst flood in Thurston County, Washington [abstract]: Geological Society of America Abstracts with Programs, v. 40, no. 1, p. 70.

Pease, M. H., Jr.; Hoover, L., Jr., 1957, Geology of the Doty-Minot Peak area, Washington: U.S. Geological Survey Oil and Gas Investigations Map OM-188, 1 sheet, scale 1:62,500. [http://pubs.er.usgs.gov/publication/om188]

Petrus, J. A.; Kamber, B. S., 2012, VizualAge: A novel approach to laser ablation ICP-MS U-Pb geochronology data reduction: Geostandards and Geoanalytical Research, v. 36, no. 3, p. 247–270. [https://doi.org/10.1111/j.1751-908X.2012.00158.x]

Phillips, W. M.; Walsh, T. J.; Hagen, R. A., 1989, Eocene transition from oceanic to arc volcanism, southwest Washington. *In* Muffler, L. J. P.; Weaver, C. S.; Blackwell, D. D., editors, Proceedings of workshop XLIV—Geological, geophysical, and tectonic setting of the Cascade Range: U.S. Geological Survey Open-File Report 89-178, p. 199–256. [http://pubs.er.usgs.gov/publication/ofr89178]

Polenz, Michael; Favia, J. G.; Hubert, I. J.; Legorreta Paulín, Gabriel; Cakir, Recep, 2015, Geologic map of the Port Ludlow and southern half of the Hansville 7.5-minute quadrangles, Kitsap and Jefferson Counties, Washington: Washington Division of Geology and Earth Resources Map Series 2015-02, 1 sheet, scale 1:24,000, 40 p. text. [http://www.dnr.wa.gov/publications/ger_ms2015-02_geol_map_port_ludlow_hansville_24k.zip]

Polenz, Michael; Gordon, H. O.; Hubert, I. J.; Contreras, T. A.; Patton, A. I.; Legorreta Paulín, Gabriel; Cakir, Recep, 2014, Geologic map of the Center 7.5-minute quadrangle, Jefferson County, Washington: Washington Division of Geology and Earth Resources Map Series 2014-02, 1 sheet, scale 1:24,000, with 35 p. text. [http://www.dnr.wa.gov/Publications/ger_ms2014-02_geol_map_center_24k.zip]

Polenz, Michael; Miller, B. A.; Davies, Nigel; Perry, B. B.; Hughes, J. F.; Clark, K. P.; Walsh, T. J.; Tepper, J. H.; Carson, R. J., 2012a, Analytical data from the Hoodsport 7.5-minute quadrangle, Mason County, Washington—Supplement to Open File Report 2011-3: Washington Division of Geology and Earth Resources Open File Report 2011-4, 42 p. [http://www.dnr.wa.gov/Publications/ger_ofr2011-4_hoodsport_supplement.pdf]

Polenz, Michael; Ostrom, B. A.; Lau, T. R.; Sadowski, A. J.; Blanks-Bennett, A. L.; Cakir, Recep; Tepper, J. H.; Legoretta Paulín, Gabriel; Nesbitt, Elizabeth; DuFrane, S. A., 2018, Geologic map of the Violet Prairie 7.5-minute quadrangle, Thurston and Lewis Counties, Washington: Washington Geological Survey Map Series 2018-04, 1 sheet, scale 1:24,000, 41 p. text. [http://www.dnr.wa.gov/publications/ger_ms2018-04_geol_map_violet_prairie_24k.zip]

Polenz, Michael; Petro, G. T.; Contreras, T. A.; Stone, K. A.; Legorreta Paulin, Gabriel; Cakir, Recep, 2013, Geologic map of the Seabeck and Poulsbo 7.5-minute quadrangles, Kitsap and Jefferson Counties, Washington: Washington Division of Geology and Earth Resources Map Series 2013-02, 1 sheet, scale 1:24,000, with 39 p. text. [http://www.dnr.wa.gov/Publications/ger_ms2013-02_geol_map_seabeck-poulsbo_24k.zip]

Polenz, Michael; Spangler, Eleanor; Fusso, L. A.; Reioux, D. A.; Cole, R. A.; Walsh, T. J.; Cakir, Recep; Clark, K. P.; Tepper, J. H.; Carson, R. J.; Pileggi, Domenico; Mahan, S. A., 2012b, Geologic map of the Brinnon 7.5-minute quadrangle, Jefferson and Kitsap Counties, Washington: Washington Division of Geology and Earth Resources Map Series 2012-02, 1 sheet, scale 1:24,000, with 47 p. text. [http://www.dnr.wa.gov/Publications/ger_ms2012-02_geol_map_brinnon_24k.zip]

Polenz, Michael; Toth, C. H.; Samson, Catherine; Sadowski, A. J.; Becerra, R. I.; Lau, T. R.; Anderson, M. L.; Nesbitt, E. A.; Tepper, J. H.; DuFrane, S. A.; Legorreta Paulín, Gabriel, 2019, Geologic map of the Rochester 7.5-minute quadrangle, Thurston and Lewis Counties, Washington: Washington Geological Survey Map Series 2019-02, 1 sheet, scale 1:24,000. [http://www.dnr.wa.gov/publications/ger_ms2019-02_geol_map_rochester_24k.zip]

Polenz, Michael; Vermeer, J. L.; Legorreta Paulín, Gabriel; Tepper, J. H.; Mahan, S. A.; Cakir, Recep, 2017, Geologic map of the Littlerock 7.5-minute quadrangle, Thurston County, Washington: Washington Geological Survey Map Series 2017-01, 1 sheet, scale 1:24,000, 36 p. text. [http://www.dnr.wa.gov/publications/ger_ms2017-01_geol_map_littlerock_24k.zip]

Pringle, P. T.; Goldstein, B. S., 2002, Deposits, erosional features, and flow characteristics of the late-glacial Tanwax Creek–Ohop Creek Valley flood—A likely source for sediments composing the Mima Mounds, Puget Lowland, Washington [abstract]: Geological Society of America Abstracts with Programs, v. 34, no. 5, p. A-89.

Reedy, T. J.; von Dassow, Wesley; Anderson, Megan; Lau, Todd; Cakir, Recep; Steely, Alexander, 2019, Neotectonic investigation of the Chehalis Basin, Southwest Washington, USA [abstract]: Seismological Society of America Annual Meeting.

Reidel, S. P., 2005, A lava flow without a source: The Cohassett flow and its compositional components, Sentinel Bluffs Member, Columbia River Basalt Group: Journal of Geology, v. 113, no. 1, p. 1–21. [https://doi.org/10.1086/425966]

Roberts, A. E., 1958, Geology and coal resources of the Toledo–Castle Rock district, Cowlitz and Lewis Counties, Washington: U.S. Geological Survey Bulletin 1062, 71 p., 6 plates. [https://pubs.er.usgs.gov/publication/b1062]

Sadowski, A. J.; Becerra, R. I.; Toth, C. H.; Polenz, Michael; Anderson, M. L.; Lau, T. R.; Nesbitt, E. A.; Tepper, J. H.; DuFrane, S. A., 2019, Geologic map of the Adna 7.5-minute quadrangle, Lewis County, Washington: Washington Geological Survey Map Series 2019-01, 1 sheet, scale 1:24,000. [http://www.dnr.wa.gov/publications/ger_ms2019-01_geol_map_adna_24k.zip]

Sadowski, A. J.; Keller, W. E.; Polenz, Michael; Lau, T. R.; Cakir, Recep; Nesbitt, Elizabeth; Tepper, J. H.; DuFrane, S. A.; Legoretta Paulín, Gabriel, 2018, Geologic map of the Centralia 7.5-minute quadrangle, Lewis County, Washington: Washington Geological Survey Map Series 2018- 05, 1 sheet, scale 1:24,000, 43 p. text. [http://www.dnr.wa.gov/publications/ger_ms2018-05_geol_map_centralia_24k.zip]

Sherrod, B. L.; Blakely, R. J.; Weaver, C. S.; Kelsey, H. M.; Barnett, Elizabeth; Liberty, Lee; Meagher, K. L.; Pape, Kristin, 2008, Finding concealed active faults: Extending the southern Whidbey Island fault across the Puget Lowland, Washington: Journal of Geophysical Research, v. 113, no. B5. [https://doi.org/10.1029/2007JB005060]

Sinclair, K. A.; Hirschey, S. J., 1992, A hydrogeologic investigation of the Scatter Creek/Black River area, southern Thurston County, Washington State: Evergreen State College Master of Environmental Studies thesis, 192 p., 8 plates. [https://salishsearestoration.org/images/b/bb/Hirschey_%26_Sinclair_1992_hydrogeology_scatter_creek_black_river_thesis.pdf]

Sláma, Jiří; Košler, Jan; Condon, D. J.; Crowley, J. L.; Gerdes, Axel; Hanchar, J. M.; Horstwood, M. S. A.; Morris, G. A.; Nasdala, Lutz; Norberg, Nicholas; Schaltegger, Urs; Schoene, Blair; Tubrett, M. N.; Whitehouse, M. J., 2018, Plešovice zircon—A new natural reference material for U-Pb and Hf isotopic microanalysis: Chemical Geology, v. 249, no. 1-2, p. 1–35. [https://doi.org/10.1016/j.chemgeo.2007.11.005]

Snavely, P. D., Jr.; Brown, R. D., Jr.; Roberts, A. E.; Rau, W. W., 1958, Geology and coal resources of the Centralia-Chehalis district, Washington, with a section on microscopical character of Centralia-Chehalis coal, by J. M. Schopf: U.S. Geological Survey Bulletin 1053, 159 p., 6 plates. [http://pubs.er.usgs.gov/usgspubs/b/b1053]

Sun, S.; McDonough, W. F., 1989, Chemical and isotopic systematics of oceanic basalts: Implications for mantle composition and processes. *In* Saunders, A.D.; Norry, M. J., editors, Magmatism in the ocean Basins: Geological Society of London Special Publication 42, p. 313–345. [https://doi.org/10.1144/GSL.SP.1989.042.01.19]

Troost, K. G., 2016, Chronology, lithology and paleoenvironmental interpretations of the penultimate ice-sheet advance into the Puget Lowland, Washington State: University of Washington Doctor of Philosophy thesis, 239 p.

Troost, K. G.; Booth, D. B., 2008, Geology of Seattle and the Seattle area, Washington. *In* Baum, R. L.; Godt, J. W.; Highland, L. M., editors, Landslides and engineering geology of the Seattle, Washington, area: Geological Society of America Reviews in Engineering Geology XX, p. 1-35. [http://www.wou.edu/las/physci/taylor/g473/seismic_hazards/troost_booth_2008_geo_seattle.pdf]

Upham, Warren, 1904, Glacial and modified drift in and near Seattle, Tacoma, and Olympia: American Geologist, v. 34, no. 4, p. 203–214.

U.S. Geological Survey Geologic Names Committee, 2010, Divisions of geologic time—Major chronostratigraphic and geochronologic units: U.S. Geological Survey Fact Sheet 2010-3059, 2 p. [http://pubs.usgs.gov/fs/2010/3059/]

Walker, J. D.; Geissman, J. W., compilers, 2009, Geologic time scale: Geological Society of America, 1 p. [http://www.geosociety.org/science/timescale/timescl.pdf]

Wallace, E. F.; Molenaar, Dee, 1961, Geology and ground-water resources of Thurston County, Washington, volume 1: Washington Division of Water Resources Water Supply Bulletin 10, v. 1, 254 p., 2 plates. [http://www.ecy.wa.gov/programs/eap/wsb/wsb_All.html]

Van Winkle, K. E. H., 1918, Paleontology of the Oligocene of the Chehalis Valley, Washington: University of Washington Publications in Geology, v. 1, no. 2, p. 69-97. [http://www.archive.org/details/paleontologyofol00palmrich]

von Dassow, Wesley; Reedy, Tabor; Anderson, Megan; Lau, Todd; Cakir, Recep; Steely, A. N., 2019, Characterization and neotectonic investingation of the trench-normal Doty fault, Chehalis basin, SW Washington, USA: [abstract] Geological Society of America Abstracts with Programs, v. 51, no. 4, p. 23.

Walsh, T. J.; Korosec, M. A.; Phillips, W. M.; Logan, R. L.; Schasse, H. W., 1987, Geologic map of Washington—Southwest quadrant: Washington Division of Geology and Earth Resources Geologic Map GM-34, 2 sheets, scale 1:250,000, with 28 p. text. [http://www.dnr.wa.gov/publications/ger_gm34_geol_map_sw_wa_250k.pdf]

Walsh, T. J.; Logan, R. L., 2005, Geologic map of the East Olympia 7.5-minute quadrangle, Thurston County, Washington: Washington Division of Geology and Earth Resources Geologic Map GM-56, 1 sheet, scale 1:24,000. [http://www.dnr.wa.gov/Publications/ger_gm56_geol_map_eastolympia_24k.pdf]

Washington Public Power Supply System, 1974, WPPSS Nuclear Project no. 3—Preliminary safety analysis report, Volume 3B: Washington Public Power Supply System, 1 v.

Weaver, C. E., 1937, Tertiary stratigraphy of western Washington and northwestern Oregon: University of Washington Publications in Geology, v. 4, 266 p. [http://babel.hathitrust.org/cgi/pt?id=uc1.b3666455;view=1up;seq=5]

Weaver, C. E., 1943, Paleontology of the marine Tertiary formations of Oregon and Washington: University of Washington Publications in Geology, v. 5, 3 parts, 789 p. [https://catalog.hathitrust.org/Record/002102073]

Weaver, C. E.; Palmer, K. V. W., 1922, Fauna from the Eocene of Washington: University of Washington Publications in Geology, v. 1, no. 3, 55 p.

Wells, Ray; Bukry, David; Friedman, Richard; Pyle, Doug; Duncan, Robert; Haeussler, Peter; Wooden, Joe, 2014, Geologic history of Siletzia, a large igneous province in the Oregon and Washington Coast Range: Correlation to the geomagnetic polarity time scale and implications for a long-lived Yellowstone hotspot: Geosphere, v. 10, no. 4, p. 692–719. [https://doi.org/10.1130/GES01018.1]

Wells, R. E.; McCaffrey, Robert, 2013, Steady rotation of the Cascade arc: Geology, v. 41, no. 9, p. 1027–1030. [https://doi.org/10.1130/G34514.1]

Wells, R. E.; Sawlan, M. G., 2014, Preliminary geologic map of the eastern Willapa Hills, Cowlitz, Lewis, and Wahkiakum Counties, Washington: U.S. Geological Survey Open-File Report 2014-1063, 2 sheets, scale 1:50,000. [http://pubs.er.usgs.gov/publication/ofr20141063]

Wells, R. E.; Weaver, C. S.; Blakely, R. J., 1998, Fore-arc migration in Cascadia and its neotectonic significance: Geology, v. 26, no. 8, p. 759–762. [https://doi.org/10.1130/0091-7613(1998)026<0759:FAMICA>2.3.CO;2]

Weigle, J. M.; Foxworthy, B. L., 1962, Geology and ground-water resources of west-central Lewis County, Washington: Washington Division of Water Resources Water Supply Bulletin 17, 248 p., 5 plates. [http://www.ecy.wa.gov/programs/eap/wsb/wsb_All.html]